DEFENSE TECHNICAL INFORMATION CENTER

Information for the Defense Community

DTIC® has determined on 7/19/2010 that this Technical Document has the Distribution Statement checked below. The current distribution for this document can be found in the DTIC® Technical Report Database.

☒ **DISTRIBUTION STATEMENT A.** Approved for public release; distribution is unlimited.

☐ **© COPYRIGHTED**; U.S. Government or Federal Rights License. All other rights and uses except those permitted by copyright law are reserved by the copyright owner.

☐ **DISTRIBUTION STATEMENT B.** Distribution authorized to U.S. Government agencies only (fill in reason) (date of determination). Other requests for this document shall be referred to (insert controlling DoD office)

☐ **DISTRIBUTION STATEMENT C.** Distribution authorized to U.S. Government Agencies and their contractors (fill in reason) (date of determination). Other requests for this document shall be referred to (insert controlling DoD office)

☐ **DISTRIBUTION STATEMENT D.** Distribution authorized to the Department of Defense and U.S. DoD contractors only (fill in reason) (date of determination). Other requests shall be referred to (insert controlling DoD office).

☐ **DISTRIBUTION STATEMENT E.** Distribution authorized to DoD Components only (fill in reason) (date of determination). Other requests shall be referred to (insert controlling DoD office).

☐ **DISTRIBUTION STATEMENT F.** Further dissemination only as directed by (inserting controlling DoD office) (date of determination) or higher DoD authority.

Distribution Statement F is also used when a document does not contain a distribution statement and no distribution statement can be determined.

☐ **DISTRIBUTION STATEMENT X.** Distribution authorized to U.S. Government Agencies and private individuals or enterprises eligible to obtain export-controlled technical data in accordance with DoDD 5230.25; (date of determination). DoD Controlling Office is (insert controlling DoD office).

Temple University
Department of Physics
Barton Hall, 1900 N. 13th Street
Philadelphia, PA 19122

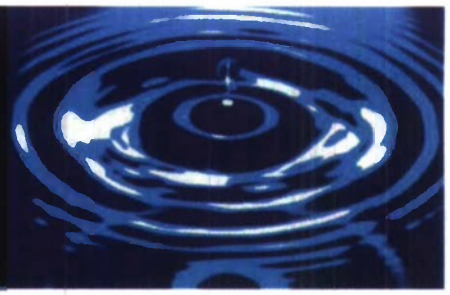

Atomic Tailoring of the Solid State Materials for Laser Cryogenic Coolers

Zameer Hasan

April 2010
Grant No. FA9550-05-1-0339

Final Performance Report
Unclassified

REPORT DOCUMENTATION PAGE

1. REPORT DATE *(DD-MM-YYYY)*	2. REPORT TYPE	3. DATES COVERED *(From - To)*
15/04/2010	FINAL	15/05/2005 - 30/11/2009

4. TITLE AND SUBTITLE

Atomic tailoring of the Solid State Materials for Solid State Coolers

5a. CONTRACT NUMBER
FA9550-05-1-0339

5b. GRANT NUMBER

5c. PROGRAM ELEMENT NUMBER

6. AUTHOR(S)

Zameer U. Hasan

5d. PROJECT NUMBER

5e. TASK NUMBER

5f. WORK UNIT NUMBER

7. PERFORMING ORGANIZATION NAME(S) AND ADDRESS(ES)

Temple University
Department of Physics
Barton Hall, 1900 N. 13th Strect
Philadelphia, PA 19122

8. PERFORMING ORGANIZATION

231365971

9. SPONSORING / MONITORING AGENCY NAME(S) AND ADDRESS(ES)

RSE

875 North Randolph Street
Suite 325 Room 3112
Arlington, VA 22203-1768

10. SPONSOR/MONITOR'S ACRONYM(S)

AFOSR

11. SPONSOR/MONITOR'S REPORT NUMBER(S)

12. DISTRIBUTION / AVAILABILITY STATEMENT

13. SUPPLEMENTARY NOTES

14. ABSTRACT

Erbium-based solid state matcrials are particularly important for low temperature laser cooling down to a few degrees Kelvin. This investigator proposed possible use of erbium-based solids for laser cooling. As of the date of this report, temperatures in bulk materials have been lowered by six dcgrees Kelvin from the ambient. This is an order of magnitudc improvement and was achieved in atomically tailored materials. Such materials incorporated two to three orders of magnitude higher concentration of erbium than used by other groups. It is significant as the cooling was observed in the weakest transition of erbium. A much stronger 1.5 micron transition commonly used for lasers in communications, is expeeted to show correspondingly higher cooling effieieneies and lower cooling temperatures. Therefore, a thinfilm cooling deviee ean be envisaged; such as a diode laser pumping a thinfilm of erbium-based material. A device like this will bring laser refrigeration to "cooling on a chip" level, revolutionizing science and technology, and establishing a new paradigm for miniaturization of devices. This report describes progress of a comprehensive research program starting with theoretical calculations to predict the cooling efficiencies; fabrication, growth and characterization of high concentration materials and most importantly performing experiments on laser cooling.

15. SUBJECT TERMS

16. SECURITY CLASSIFICATION OF:			17. LIMITATION OF ABSTRACT	18. NUMBER OF PAGES	19a. NAME OF RESPONSIBLE PERSON
a. REPORT	b. ABSTRACT	c. THIS PAGE			ZAMEER U. HASAN
UNCLASSIFIED	UNCLASSIFIED	UNCLASSIFIED		95	19b. TELEPHONE NUMBER *(include area code)* (215) 204 2733

Standard Form 298 (Rev. 8-98)

Atomic Tailoring of the Solid State Materials for Laser Cryogenic Coolers

Zameer Hasan
April 2010
Grant No. FA9550-05-1-0339

Temple University
Department of Physics
Barton Hall, 1900 N. 13th Street
Philadelphia, PA 19122

Abstract

Erbium-based solid state materials are particularly important for low temperature laser cooling down to a few degrees Kelvin. This investigator proposed possible use of erbium-based solids for laser cooling. As of the date of this report, temperatures in bulk materials have been lowered by six degrees Kelvin from the ambient. This is an order of magnitude improvement and was achieved in atomically tailored materials. Such materials incorporated two to three orders of magnitude higher concentration of erbium than used by other groups. It is significant as the cooling was observed in the weakest transition of erbium. A much stronger 1.5 micron transition commonly used for lasers in communications, is expected to show correspondingly higher cooling efficiencies and lower cooling temperatures. Therefore, a thinfilm cooling device can be envisaged; such as a diode laser pumping a thinfilm of erbium-based material. A device like this will bring laser refrigeration to "cooling on a chip" level, revolutionizing science and technology, and establishing a new paradigm for miniaturization of devices. This report describes progress of a comprehensive research program starting with theoretical calculations to predict the cooling efficiencies; fabrication, growth and characterization of high concentration materials (up to 100% rare earth) and most importantly performing experiments on laser cooling.

Contents

List of Figures

Acknowledgement

The author would like to aeknowledge his family and friends to allow him for a long leave of absence from himself during the course of this work. Some students of him also patiently waited for their share of time while he was busy in the laboratory. Most noteworthy among them are Franeiseo Bezares, Mike Companell and Adam Adamezyk.

The students who believed that we could do it are very special. Zhengle Qiu and Jonathan Lyneh deserve special reeognition. Mses. Janis Zambrano and Elcanor Cicinsky and Professor Leroy Dubeck went out of their way to cireumvent many teehnical and administrative problems.

Most importantly, this work was introduced and initiated by the Air Foree Offiee of Scientific Research. It was made possible by a grant from them. I greatly appreciate their patience at every level and throughout the course of this investigation.

1. Summary

Realizing optical cooling in erbium-based solids was the major purpose of these investigations. This report presents results of bulk cooling in erbium-based solids in this laboratory in the 0.8 micron region. This investigation has observed cooling of a crystal by more than six degrees Kelvin. This cooling was observed in the most forbidden transition of erbium where the least cooling was expected.

Since this proposal, cooling in erbium has been confirmed by Fernandez et. al. in 2006. Fernandez reported cooling in the 0.8 micron region for one crystal and one glass host. However, this transition was the weakest of erbium transitions which resulted in inefficient cooling and the sample temperatures were lowered by only a fraction of a degree Kelvin in a localized region. Cooling in the 1.5 micron infrared transition of erbium was observed at Naval Research Laboratory in 2008. Although the absorption strength of this transition is five orders of magnitude stronger in comparison to the 0.8 micron transition, the team at the Naval Research Laboratory observed cooling of only a few hundredths of a degree. Coolers based on the 1.5 micron transition have the potential for providing much lower temperatures and higher efficiencies. Further, this transition of erbium is in a region of the spectrum that is safe to the human eye. Lastly and most importantly, pump lasers required for 1.5 micron optical coolers have been commercially well developed. This is due to the fact that 1.5 micron lasers and amplifiers of erbium have been the workhorse of photonics and communication technologies for the last three decades.

In order to improve upon the efficiency of cooling of erbium based solids, this research program has focused on atomically tailoring the electronic and thermal or vibrational properties of materials. Such materials were fabricated and then cooling experiments were performed on them. There were three different but related areas of investigation that converged to yield the laser cooling results presented here. This report, therefore, presents the status of progress in each of these areas:

1. Theoretical Calculations: Theoretical calculations have been performed for erbium electronic energy levels in chloro-elpasolite crystals. These calculations gave electronic energies

and wavefunctions in the presence of a cubic crystal field. From these wavefunctions the strengths of optical transitions were calculated. Based on these calculations, the absorption characteristics in the infrared and the visible region of the spectrum have been modeled and predicted from first principle. Experimentally observed absorption spectra have been found to follow the calculated intensities very closely. This establishes the predictability of cooling efficiencies on the basis of theoretical calculations for various transitions in erbium. A significant outcome of these calculations is that the 1.5 micron transition of erbium was established to be more than five orders of magnitude stronger than the transition at 0.8 micron, for which cooling results are reported in this report. It is anticipated that with proper atomic tailoring of crystal field energy levels and wavefunctions for the 1.5 micron transition a correspondingly higher efficiency of cooling and lower temperature will be achieved.

2. Fabrication: This group has worked to fabricate and grow the materials investigated in part 1 with higher concentrations of erbium. Towards this goal, crystals with concentrations ranging from 5% to 100% erbium allowed by the chemical formula have been grown and characterized for laser cooling.

3. Laser Cooling Experiments: To investigate these systems for laser cooling, a versatile experimental station has been built. This experimental station is based on a high vacuum chamber for the sample and includes three setups for independently monitoring laser cooling using different experimental techniques:

A. Laser cooling setup using high sensitivity dual thermocouple probe: Ultra-sensitive thermocouple junctions are used to monitor any temperature changes upon laser irradiation of the sample. One probe monitors the change in crystal temperature and the other is used to monitor the changes in the temperature of the chamber in the vicinity of the sample.

B. Laser cooling setup using high sensitivity photo-thermal deflection: In this case, a probe laser passes through the crystal and monitors its temperature changes by monitoring the changes in the refractive index of the crystal. Changes of the refractive index are measured by the deflection of the probe Helium-Neon laser.

C. Laser cooling setup using fluorescence line narrowing: These measurements monitor the crystal temperature by measuring the narrowing of rare earth spectral lines. It is built around a grating spectrograph and sensors in the IR and visible regions of the spectrum.

In conclusion, our experiments have shown orders of magnitude improvement in cooling of erbium-based solids using the weakest transition of erbium. The potential for further enhancement of cooling is not only theoretically favorable and commercially viable, but also experimentally possible. Research presented here is the proof of concept needed to justify further experimentation.

Compact laser coolers would enhance many DOD capabilities such as remote sensing, surveillance, reconnaissance and target recognition. All such applications require gathering, storage and processing of massive amounts of data and better discrimination of targets by sensors. Fast and compact processors and ultra-high density memories as well as compact arrays of IR sensors could all use a compact and integrated array of optical refrigerators for their best performance. It would also greatly reduce the payload of airborne and space missions.

2. Personnel Supported

Faculty

Dr. Zameer Hasan	Principal Investigator, supported for one to two months summer salaries 2005-2008

Post Doctoral Fellows

Dr. Hikmat Najafov	Full time, September 2006-June 2007
Dr. Imran Khan	Full-time, April 2009-November 2009
Dr. Moniruzzaman Syed	Part time, September 2005-November 2005

Graduate Students

Mr. Joseph Palma	Full time Research Assistant, 2005-2007
Mr. Zhengle Qiu	Part time Research Assistant, Summers 2005-2009
Mr. Jonathan Lynch	Part time Research Assistant, Summer 2009
Dr. Francisco Bezares	Part time Research Assistant, Summer 2007-2009
Dr. Aras Konjhodzic	Part time Research Assistant, 2007-2008
Dr. Mohamed Aly	Part time Research Assistant, Summer 2005
Mr. David Barton	Part time Research Assistant, Summer 2006
Mr. Adam Adamczyk	Part time Research Assistant, Summer 2005-2006

Undergraduate Students

Mr. Mike Campanell	Partially financially supported for one summer
Ms. Lily Nguyen	Partially financially supported for one summer
Mr. Emmanuel Vassilarakis	Not financially supported
Ms. Ariel Wallace	Not financially supported

Mr. Paul Soldate	Not financially supported

Doctoral Thesis Completed or in Progress

Dr. Francisco Bezares	Completed in December 2009, thesis available from Physics Department, Temple University
Dr. Aras Konjhodzic	Completed Spring 2008, thesis available from Physics Department, Temple University
Mr. Zhengle Qiu	Thesis in progress: Rare Earth Doped Materials for Laser Refrigeration
Mr. Jonathan Lynch	Thesis in progress: Laser Cooling in Erbium Based Solid State Materials

3. Introduction

It was more than eighty years ago when Peringsheim [1] forwarded the idea that a solid could be cooled by radiation. If a solid is made to emit photons of energy higher than it absorbs from the incident radiation field a net cooling of the solid can be achieved. This proposition was disputed even by the brightest minds of that time as a thermodynamic impossibility [2-3] until 1946 when Landau [4] showed that Peringsheim was correct. He pointed out that the source of cooling radiation, such as a laser in modern experiment, should also be taken into consideration, then overall entropy of the closed system, laser and the solid, increases even when the temperature of the solid decreases. Naturally, the advent of laser provided a monochromatic powerful source of radiation and gave an impetus to research activities in this direction [5-6]. However, many attempts to cool solids, spanning approximately three decades following the advent of laser, did not provide any positive result from laser cooling [7]. The first conclusive observation of cooling in a solid was reported in 1995 by Epstein et. al. [8] where cooling of a solid by 0.3 Celsius (or Kelvin) from the ambient temperature was achieved.

In the past fifteen years following the first reported cooling of a solid, there has been great progress in laser refrigeration. Bulk materials have been cooled down to 208 K and laser refrigerators with highly pure crystals have recently passed the thermo-electric coolers limit for cooling. Applications of laser refrigeration in technology at sub-liquid nitrogen or liquid helium temperatures will undoubtedly revolutionize our world. It will reduce the size of electronic devices to close to atomic sizes and will make remote freezing of objects possible.

Although there have been many proposals for laser cooling of solids in semiconductors and transition metal based systems, it has been most successfully demonstrated in rare earth

based solid-state materials. Among the fourteen rare earth lanthanides only three, when incorporated in a solid, have been shown to exhibit cooling. Ytterbium in ZBLAN or ZBLANP glass has yielded the best results lowering temperatures by as much as 208 K [9] or better in bulk materials. Ytterbium's success is followed by Thulium [10-20]. In both cases, internal efficiencies in excess of 90% have been achieved by Epstein and Sheik-Bahae, [21-22] in their research groups at Los Alamos National Laboratory and the University of New Mexico.

Erbium is the third rare earth ion where laser cooling has been conclusively demonstrated. Prior to the proposal for the present investigations, erbium based solids were not considered suitable for laser cooling. It was believed that due to a complex energy level scheme of erbium, upon irradiation with a laser, many optical processes would compete with a net result of heating rather than cooling. We argued that with proper tailoring of electronic and vibrational states a net cooling might be possible. In results reported here, cooling by more than 6 degrees Kelvin has been observed.

In addition to the present investigation there have been two more reports of cooling in Er-based systems. Cooling was first reported by Fernandez et. al. [23] and later at the Naval Research Laboratory in Bowman's group [24]. Two different transitions have been used by these groups, one in 0.8 micron range for pumping the $^4I_{9/2}$ state and the other pumping the $^4I_{15/2}$ - $^4I_{13/2}$ transition at 1.5 microns. In both cases, the efficiencies of cooling were very low, ~ 0.1-0.38%, and cooling of bulk materials by ~ 0.7 °C and 0.03 °C were demonstrated. This report presents results showing the lowering of temperatures by almost an order of magnitude greater than reported by Fernandez and two orders of magnitude greater than reported by Bowman's group. This increase is mainly due to the use of crystals tailored to have a higher concentration

of erbium, about two orders of magnitude higher, than used elsewhere. It is significant that this order of magnitude increase in cooling was observed in the weakest transition of Erbium at 0.8 micron. The well known 1.5 micron transition is the strongest transition and holds better promise for cooling.

There are many advantages of using Erbium for laser cooling purposes. One such advantage is that for cooling involving the 1.5 micron transition, the communication lasers can be used as cooling lasers. This is a great advantage, as for any laser cooling material; the laser wavelength must be tailored to the energy level scheme of the electronic transitions involved. The specificity of the cooling laser is particularly severe for rare earths because the 4f-4f electronic transitions are very sharp in energy, and lasers developed for one rare earth or even a specific transition in it, cannot be used for any other cooling transition.

Furthermore, Er-lasers for communication are well developed. Thinfilms diode lasers are generally used to pump them. With an efficient high concentration erbium cooler, the cooling medium can be reduced to a thin film. Thus, the entire system: pump laser, cooling laser, and the cooling material can be, in principle, combined on a chip. Therefore, a thin film cooling device based on multi-layer structures can be envisaged, Figure 1. Obviously, such a device can cool only a small amount of material. However, in most applications only a small amount of material needs to be cooled. Because of the ever-decreasing size of devices, materials weighing in the micrograms or even smaller amount need to be cooled. Thus, by making the cooling device comparable in size to the materials to be cooled, one can eliminate bulky cryogenics and bring

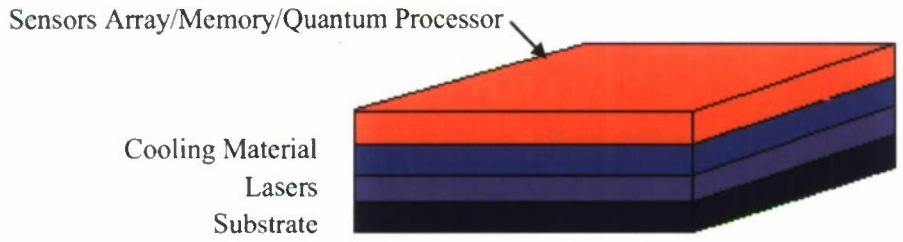

Figure 1. Schematics of a multi-layer thinfilm laser refrigerator and the device to be cooled, such as sensors, memory or a processor

cooling where it is needed. Such a device would also furnish a cooling laboratory on a chip where some of the most novel experiments can be performed. This will not only eliminate bulky cryogenic refrigerators used in present day experiments but will also make experiments on micro- and nano-samples a routine matter. Last but not the least, such cooling devices will certainly be more energy efficient and space conserving.

The organization of this report is as follows. First, theoretical background for laser cooling is developed in section 4, followed by general criteria that establish the choices of rare earth lanthanides and their possible atomic tailoring in section 5. Theoretical calculations of rare earths energy levels in crystals and wavefunction calculations are presented in full details for the crystals of interest. In section 6, material designing and fabrication are presented. The instrumentation for optical characterization and related experiments including laser cooling of these materials are presented in section 7. This section provides a brief description of the facilities developed for processing and fabrication of materials and experimental stations for observing laser cooling. Results of optical and laser cooling studies are presented in section 8 with conclusions of the present investigations in section 9. Section 10 briefly gives recommendations for future studies to focus on erbium refrigerators in the 1.5 micron region with the ultimate aim of making them in the form of multilayer-thin-film structure.

4. Laser Cooling in Rare Earth Doped Solids

Historically, rare earths ions in solids were the first materials suggested for cooling. Interestingly in spite of many attempts of cooling transition metal ion doped solids and semiconductors, laser cooling has thus far been observed only in rare earth doped solids. In this section a brief introduction to laser cooling in rare earth based solids will be followed by theoretical calculations for erbium in elpasolite, the system that has shown by far the best cooling of any erbium system.

To date, Laser refrigeration has been most successfully demonstrated in RE-based solids, particularly ytterbium doped in inorganic glasses (ZBLAN and ZBLANP) [21-22]. Temperatures as low as 208 K have been attained on a regular basis. In a recent report, Epstein's group at Los Alamos Laboratory and their collaborators have surpassed the limit of thermo-electric coolers in optical refrigeration RF. The size of the refrigerator has been reduced greatly to roughly the size of the human fist [25].

The physical principle of laser cooling is shown in Figure 2 (a). States 1 and 2 are ground and excited electronic states of an atom or ion in a solid. The vibrationally (or any other low energy) excited level of state 1, v_1, is shown as a narrow line. A laser excites the electrons from the thermally excited level of the ground state, v_1, taking it to excited state 2. From state 2, radiative emission to the purely electronic ground state 1 results in the energy up-conversion of the emitted photon. This additional energy comes from the lattice vibrations. Therefore, with every cycle of this process also known as anti-stokes shifted emission, the lattice loses energy and the solid cools down.

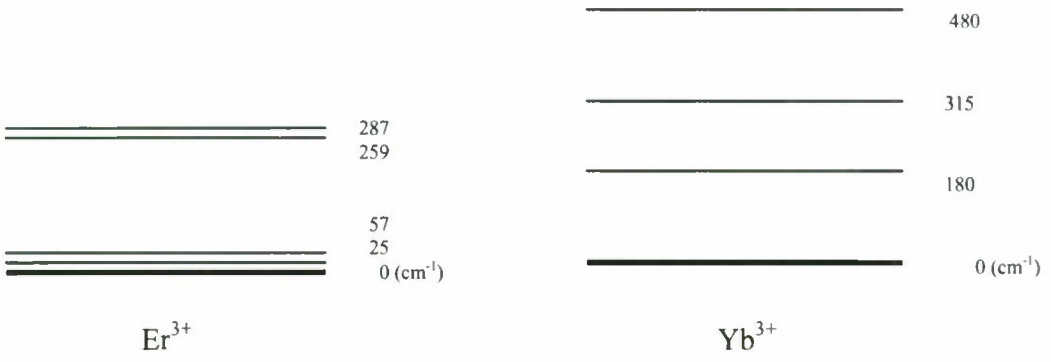

(b)

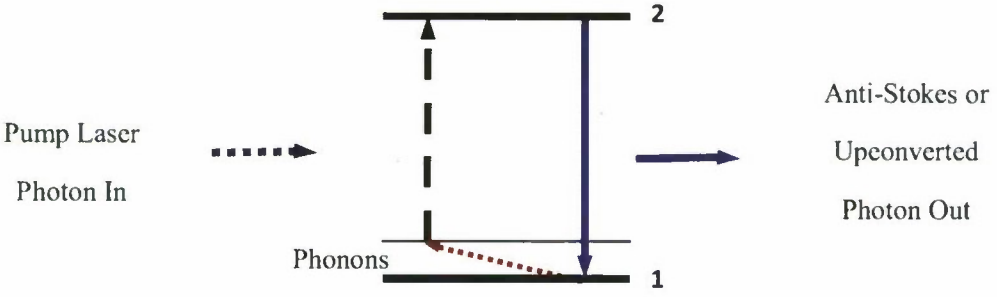

(a)

Figure 2. (a) Schematics of RE- based laser cooling. (b) Ground state splitting of Er^{3+} in elpasolite and Yb^{3+} in ZBLAN hosts. Energy separations given on the left in cm^{-1} are not drawn to scale.

The first law effieieney of eooling ean be written as:

$$\eta = \varepsilon/E \qquad (1)$$

Where ε is the phonon energy or the lattiee vibration absorbed and E is the ineident photon energy that is invested in absorbing lattiee energy ε. This simple pieture is eonsiderably eomplieated with the energy level multiplieity in any real situation, Figure 2(b), and seeondly, the energy losses that are diffieult to estimate due to optieal energy transfers and non-radiative multi-phonon relaxations [26-29].

Obviously, the question arises, why one ean't eool solids to or below liquid helium temperature. For atomie vapors, laser eooling ean bring the temperature down to miero-Kelvin and even lower. The limiting factors in solids fall into two eategories: The first eategory problems are more fundamental in nature and depend on the energy level seheme used for eooling and the host lattiee. The other eategory of problems is teehnieal in nature and mainly assoeiated with the design of the eooler, its eontaet with the objeet to be eooled, and its thermal isolation from the surrounding. These latter types of problems are by no means trivial. However, they are uniquely defined for every system and every seheme of eooling. These limiting faetors will not be dealt with here.

From Figure 2(a), it ean be seen that for effieient laser eooling, the ineoming photon from the pump laser should be strongly absorbed, the anti-stokes shifted photon should eseape from the system without being re-absorbed, and thirdly, the laser eooling medium should be able to reaeh the exeited vibrational state by absorbing one or more quanta of lattiee vibrations, as

shown by a small dotted arrow. Therefore, atomic tailoring of a laser cooling material has three main challenges:

1. Efficient absorption of incoming laser photons
2. Minimum or no re-absorption of outgoing, upconverted photons
3. Efficient populating of state v_1 by thermal vibrations of the lattice

For all of the above we need to tailor the electronic and vibrational properties at the atomic scale.

5. Atomic Tailoring of Materials

In this section we address the issues mentioned in the last section by atomic tailoring of electronic and vibrational properties of the laser-cooling medium. The ultimate goal is to achieve higher efficiency and lower temperature in laser coolers. In the following section we check the suitability of rare earth doped materials particularly the $4f^n$ lanthanides series for laser cooling.

5.1 f-f Transition in Lanthanides

In this category the *4f-4f* transitions of lanthanides provide the energy levels scheme for the cooling. There are definite advantages of such systems. First, the electronic energy level scheme is predictable. The outer *5s* and *5p* completely filled shells shield the *4f* incomplete shell of lanthanides. Therefore, optically active electrons of the *4f* shell are only slightly affected by the crystal field of the host lattice; *4f* electron energy levels and their relative separations essentially remain the same in going from one solid host to another. As in other applications, the choice of *f-f* lanthanide transitions in laser cooling is due to the predictable electron energy level scheme from one solid to another. Depending on a particular application, choices of the solid host can be made without worrying about the changes in the electronic energies of the lanthanides. Secondly, the thirteen members of the lanthanide series, starting from $Ce^{3+}(4f^1)$, to $Yb^{3+}(4f^{13})$, provide one of the richest sets of energy levels [30]. Transitions between these states extend from the far IR to the UV. For this reason, there are a variety of transition schemes for almost any application in photonics. The *f-f* optical transitions of the $4f^n$ electronic configuration are electric dipole forbidden and therefore are generally weak. This results in a weaker coupling

of the laser radiation and the *4f* electrons of lanthanide used for cooling. The magnetic dipole transitions are the next strongest and are allowed between the electronic states derived from the f^n configuration. Selection rules for these transitions are such that $\Delta J=0, \pm 1$, excluding *0-0* transitions and $\Delta l=0$. For tri-positive lanthanides, it is the most suitable class of transitions for laser cooling.

The electronic energies of the $4f^n$ configuration are only slightly affected by the crystal field. The changes amount to a few meV at the most and are smaller than the effect of the spin-orbit coupling. A more relevant change is in the symmetry of the crystal field. This changes the electronic transition selection rules. In thinfilms these changes can be tailored in one more way; by introducing an impurity at the time of fabrication. If the impurity atom or ion occupies a site close to the rare earth ion, it changes the symmetry and the magnitude of the crystal field experienced by the *4f* electrons appreciably [31-36].

The choice of lanthanide for laser cooling, to some degree, is dictated by the energy separation E between the ground and excited electronic state. It should lie in the IR region where highly efficient diode lasers are readily available. This limits the choice of laser cooling transition from dark red to the near-IR region. In the following, we present the case of individual lanthanides based on the criteria discussed above.

Ce^{3+} and Yb^{3+} have by far the simplest electronic energy level scheme for laser cooling. Both of these ions have only one electronic excited state. However, for Yb^{3+} the energy separation between the ground and the excited state, E, equation (1), is about five times larger than for Ce^{3+}. Therefore, non-radiative relaxations that involve lattice phonons to deplete the excited state will be more prevalent in Ce^{3+} in comparison to Yb^{3+}. The probability of such a

relaxation varies as $1/p^n$, where p is the probability of the process and n is the number of phonons involved in depleting the exeited state non-radiatively. The energy separation between the ground and exeited eleetronie states, E, and the phonon frequeney, ω, follow the relationship

$$E = n \hbar \omega \qquad (2)$$

Therefore, n (Yb^{3+}) = $5n$ (Ce^{3+}). At room temperature T=300 K ~210 em^{-1} roughly 10 phonons of this energy will be depleting the exeited state of Ce^{3+} where as for Yb^{3+} this number will be elose to 50.

Tm^{3+} and Ho^{3+} are other interesting ions for laser eooling. For the remaining RE^{3+} ions in the lanthanide series, the exeited eleetronie state (eorresponding to the magnetie dipole transition) is too elose to the ground state. In all these eases multi-phonon relaxations ean severely limit any radiative emission. Seeondly, pump lasers in the far IR are not so readily available.

Er^{3+} is an attractive eandidate for laser eooling. Its magnetie dipole allowed transition is at 1.5 mierons in the eye safe region. Among lanthanides, it is seeond only to Yb^{3+} on the basis of having least energy losses from multiphonon relaxations. In addition, this transition is eommonly used for deviees in optical eommunieation. Using Er^{3+} magnetie dipole transitions would enable one to employ eommunieation lasers as the pump for laser eooling. The teehnology for these lasers has been highly developed over the past twenty years. In some materials Er exeited states absorption may be an issue. We will diseuss it in detail later in seetions 6 and 8, on up-eonversion laser materials. We will show in a later seetion that the ground state multiplet of Er has low energy eleetronie levels so as to populate them by lattiee

phonons at low temperatures. This way low temperature cooling can be obtained down to 10 K or so in our material. Further tailoring of this state is possible to bring the cooling temperature further down. It is a great advantage. In comparison, Yb has much greater ground state energy separations and therefore, it has a fundamental limit of cooling ~100 K or higher, Figure 2(b). For cooling at low temperature both the low energy electronic states and low energy phonons to populate them should be present.

5.2 Tailoring Phonons/Vibrational Properties

In low temperature laser cooling, we need a high density of low energy vibrations or phonons. The vibrational spectrum of the material is another property that can be tailored for laser cooling. In going from one solid host to another, vibrational properties change significantly. Introducing impurities can also alter elastic properties, more so in the vicinity of the impurity atom. This creates vibrational modes that are localized near an impurity atom or defect in the lattice [37-39]. Another consequence of doping an impurity atom, although a second order effect in case of rare earth ions, is the change in the electronic wavefunctions due to vibrations in a dynamic crystal.

All of the above culminate into two effects relevant to laser cooling. 1) A change in the density of vibrational states. 2) A change in the electron-vibration coupling (the latter has an even greater implication for the efficiency of laser cooling). Thus, tailoring vibrational properties allows control over the selection rules of radiative transitions between the electronic and vibronic states as well as non-radiative relaxations.

For efficient laser cooling, non-radiative relaxations should be suppressed or even eliminated. Choosing materials with low energy phonons can do this. Elpasolite, the subject of most of the studies in this report is such a material. It has one of the best low energy phonon spectrum when compared to other crystals and glasses used for laser cooling. Vibrations localized around the rare earth ion make otherwise forbidden transitions allowed and carry most of the intensity in the optical spectra of cubic systems such as elpasolites [26-28, 40-45]. It is these vibrations that will facilitate carrying the lattice energy out and hence cooling the crystal, especially at low temperatures.

5.3 Erbium Electronic Energy-Level Calculations

One of the unique advantages of studying Er in elpasolites is that full crystal field calculations can be performed on this system that give electronic energy levels and wavefunctions. The wavefunctions can be used to calculate the transition strengths for various transitions of erbium. This knowledge provides us with:

- the selection of electronic transition on the energy basis;
- relative efficiency of cooling in different transitions;
- the lowest temperature possible in cooling and
- an insight for tailoring non-cubic crystals and glassy materials.

This advantage is unique to cubic systems where a minimum of crystal field parameters, only two, can be used to express the crystal field. In comparison, for $KPb_2Cl_5:Er^{3+}$ a low symmetry field further splits the energy levels that are otherwise degenerate in the cubic system. This increases the number of adjustable parameters and exact calculations and their comparisons are not possible in any non-cubic crystal.

We therefore give an outline of the calculation that was performed to determine the $4f^{11}$ electronic energy-level structure of Er^{3+} in Cs_2NaYCl_6. We used a model Hamiltonian that operated entirely within the $4f^{11}$ configuration [26, 46-49],

$$H = H_a + H_{cf} \tag{3}$$

where H_a is defined to incorporate the isotropic parts of H (including the spherically symmetric parts of the 4*f*-electron/crystal-field interactions), H_{cf} is defined to represent the non-spherically symmetric components of the one-electron crystal-field interactions.

$$H_a = E_{ave} + \sum_k F^k f_k + \alpha L(L+1) + \beta G(G_2) + \gamma G(R_7) + \xi_{s0} A_{s0} \tag{4}$$

where k=2,4,6; i=2,3,4,6,7,8; j=0,2,4; and each of the interaction operators and interaction parameters is written and defined according to standard practice. The $[SL]J$ multiplet structure of the $4f^{11}(Er^{3+})$ electronic configuration is determined predominantly by the H_a part of the model Hamiltonian, whereas mixings between different multiplets and splittings within individual multiplet manifolds are determined by the crystal-field interactions represented in H_{cf}.

The one-electron crystal-field interaction Hamiltonian (H_{cf}) employed in this study was defined to reflect the (O_h) symmetry of the Er^{3+} ions in $Cs_2NaErCl_6$, and in its parameterized form it may be written as

$$\begin{aligned} H_{cf} = {} & B_0^{(4)}[U_0^{(4)} + (5/14)^{1/2}(U_4^{(4)} + U_{-4}^{(4)})] \\ & + B_0^{(6)}[U_0^{(6)} - (7/2)^{1/2}(U_4^{(6)} + U_{-4}^{(6)})] \end{aligned} \tag{5}$$

where the $U_q^{(k)}$ are intraconfigurational spherical-tensor operators of rank k and order q, and B_0^6 and B_0^2 are one-electron crystal-field interaction parameters.

In the energy-level calculations performed in this study, the model Hamiltonian was diagonalized within the complete set of $4f^{11}SLJM_J$ angular momentum states (a total of 364

states), and various subsets of the Hamiltonian parameters were treated as variables in fitting the calculated energy levels to those located and assigned from experiment.

Results obtained from energy-level calculations with more advanced correlated crystal fields taken into consideration are shown in Table 1, along with the experimentally observed locations and symmetry assignments [29]. Of the 364 energy levels calculated, in Table 1 we have included only a few low lying energy levels relevant to laser cooling. The accuracy of these calculations is remarkable. The differences in observed and calculated electronic energies are only a few cm^{-1} at the most as seen from Figure 3. Energy levels assigned from the experimental spectra are given in the column on the right hand side.

Table 1. Calculated and observed energy levels of Er^{3+}:Cs_2NaYCl_6

Level	Multiplet Label	Crystal-field Level	Energy Calculated (cm^{-1})	Energy Observed (cm^{-1})
1	$^4I_{15/2}$	Γ_8	*0*	*0*
2		Γ_7	*24*	*25*
3		Γ_8	*58*	*57*
4		Γ_6	*257*	*259*
5		Γ_8	*290*	*287*
6	$^4I_{13/2}$	Γ_6	*6497*	*6492*
7		Γ_8	*6523*	*6517*
8		Γ_7	*6537*	*6532*
9		Γ_8	*6688*	*6682*
10		Γ_7	*6695*	*6686*
11	$^4I_{11/2}$	Γ_6	*10162*	*10166*
12		Γ_8	*10169*	*10174*
13		Γ_8	*10230*	*10238*
14		Γ_7	*10234*	*10238*
15	$^4I_{9/2}$	Γ_8	*12348*	*12345*
16		Γ_6	*12424*	*12410*
17		Γ_8	*12496*	*12489*
18	$^4F_{9/2}$	Γ_8	*15180*	*15152*
19		Γ_8	*15264*	*15246*
20		Γ_6	*15335*	*15337*

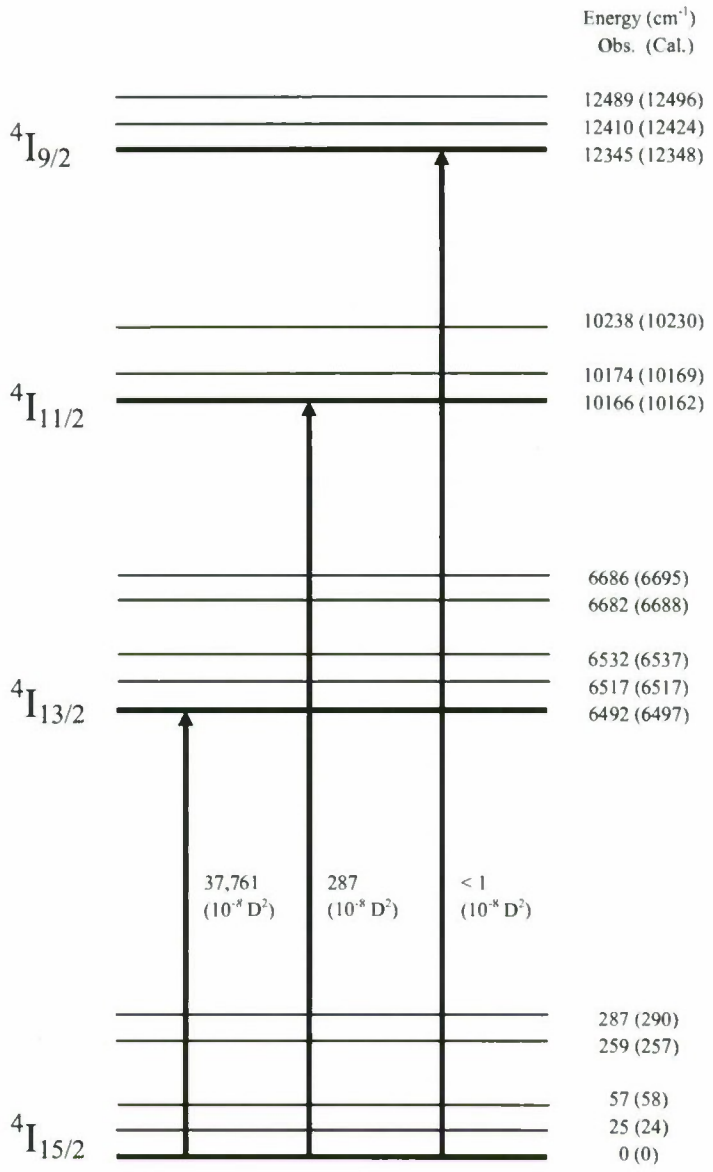

Figure 3. Calculated and observed *[LS]J* multiplets of erbium in elpasolite crystal relevant to laser cooling. The calculated energy positions are shown in parentheses in cm^{-1}. The calculated sum of absorption strengths for the transitions between the multiplets are also given in units of 10^{-8} $(Debye)^2$. Note that energy positions are not to scale.

5.4 Optical Transition Strength for Relevant Cooling Wavelengths

The wavefunctions obtained from the crystal field calculation were used to calculate and compare the strength of various optical transitions. The transition strengths are also given in Figure 3 for all transitions that are relevant to cooling in this material. It is remarkable to note that the 0.8 micron $^4I_{15/2}$ - $^4I_{9/2}$ transition where the cooling was observed in our laboratory and was also the first transition to show cooling anywhere else is the most forbidden transition. It has negligible optical strength < 1(10^{-8} D^2). This should be taken as the testimony to the potential of erbium for cooling in better known 1.5 micron transition where the optical transition strength is ~37,700 (10^{-8} D^2).

The numbers shown above are the total dipole strengths for the transitions between all crystal field states of the ground and excited multiplets. With the calculated intensities a spectrum can be simulated that very closely predicts the observed spectral positions and intensities [26].

6. Material Designing and Fabrication

In this study three different types of erbium doped materials were used. Two of them were crystals, cubic Cs_2NaYCl_6 and monoclinic KPb_2Cl_5, whereas the third was a glass well known as a suitable host for laser cooling host materials, ZBLAN (ZrF_4-BaF_2-LaF_3-AlF_3-NaF).

Crystals of KPb_2Cl_5 with nominal percentage of Er (1% by formula) were grown by the Bridgeman technique at Hampton University by Dr. Uwe Homerick. The ZBLAN glass doped with two atomic percent of Er was grown from the melt at Oak Ridge National Lab by Dr. Jackie Johnson. Among these systems only Cs_2NaYCl_6 can be grown in the stoichiometric form and erbium concentration can be varied from 0%-100%. Cs_2NaYCl_6 was the only crystal grown in our laboratory. Therefore, we will describe their procedures in detail.

6.1 Single Crystals of Er-Doped Elpasolites

Single crystals of Cs_2NaYCl_6 with erbium replacing Y as a dopant could be grown with up to 100% erbium, i.e., $Cs_2NaErCl_6$. The schematics are shown in Figure 4. These were all grown by the principle investigator in quartz ampoules using a Bridgeman furnace. The details of growth are described elsewhere [29, 50]. One particular caution to be taken with these extremely hygroscopic materials is to make sure that there are no traces of water left in the starting material. This was accomplished by passing dry HCl gas through the starting material for several hours in the dehydration chamber. The sample in the form of dry powder was then transferred to the quartz ampoules. At this stage, the ampoules were sealed using a flame from a hydro-oxy torch, these ampoules were traversed through a Bridgeman furnace kept at 950°C shown in Figure 4(b). Typical speed of passing the quartz ampoule was <1cm/hour. The whole

proeess took a week's time to grow a single batch. The crystals were stored in ampoules unless needed for the experiments and once opened required storing in evaeuated desieeators to proteet them from the ambient water traces.

6.2 Cutting and Polishing

All of the erystals studied in the present investigation were polished and eut at Temple University. For this purpose a large vaeuum glove box was built in our laboratory. Figure 5 shows this box. It has four gloved aeeess ports, two evaeuated entry ports and several gas and vaeuum lines. Thus, it ean be used by a couple of users at the same time. This arrangement never exposes the erystals to the environment. Most of the polishing and eutting of the erystals were done in this ehamber. The large glove box was equipped with a rotary pump to be able to aehieve a vaeuum of a few millitorrs. Prior to loading and unloading, several eyeles of evaeuating and filling with nitrogen gas were performed to ensure that the environment in this glove box was free of any water traees. Thus, eutting, polishing and other preparations were always performed in a dry nitrogen environment.

Another smaller ehamber was built to load the erystal and to polish it near the laser eooling ehamber of Figure 6. This smaller glove box utilized a flow of nitrogen to ereate the water free and elean environment and therefore was not as free of water traees as the large glove box.

Cutting and polishing were performed using mineral oil as a eoolant as well the medium for the lapping paste. Polishing invariably used either diamond or aluminum oxide powder; diamond paste in ease of glass and aluminum oxide for erystals that were softer than glass.

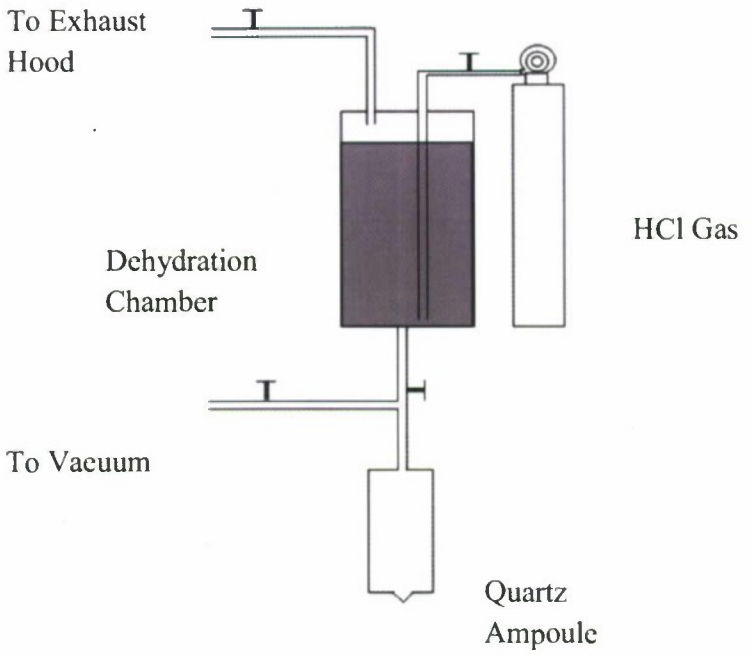

(a)

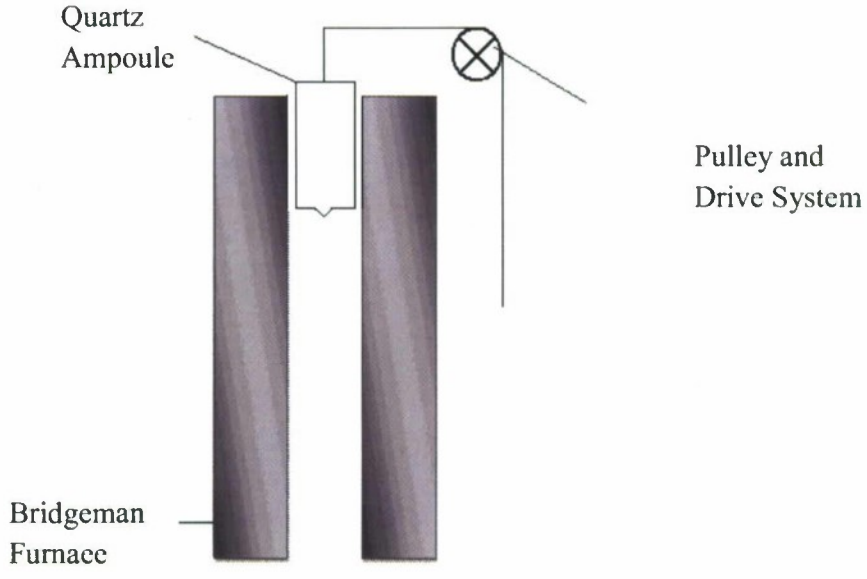

(b)

Figure 4. Crystal Preparation: (a) Dehydration by HCl gas; (b) Crystal growth in Bridgeman furnace. The quartz ampoule is lowered in the furnace with a typical rate of 1 cm/hour.

Figure 5. Vacuum chamber and glove box built for handling the hygroscopic crystals. All cutting and polishing were performed in this chamber.

Figure 6. Glove box for mounting the sample in the vacuum chamber for laser cooling. The mounting is carried out in nitrogen atmosphere to avoid ambient water traces.

7. Optical Techniques and Characterization

Typical concentrations of rare earth impurities in our samples ranged from ~ 0.01 mol % to 100% allowed by the chemical formula, i.e. fully stoichiometric. Optical characterization is the only way to determine the presence of the appropriate rare earth centers in the sample with desirable concentration. This is particularly true for the solid hosts that allow for multiple optical centers associated with a RE- impurity. The types of optical measurements performed on the sample were absorption studies, using Cary 500, emission and lifetime studies on optical systems built in-house. Low temperature emission and selective excitation were found to be the most powerful techniques in determining the presence of the desired RE optical-center. The lifetime measurement provided complimentary information for the ultimate characterization of samples.

7.1 Experimental Procedures for Optical Studies

Commercially available instruments were used only for low-resolution absorption experiments that were essential for optical characterization of cooling materials. For all other optical investigations on these systems, particularly at high-energy resolutions, experimental setups were designed in-house using commercially available components such as lasers, detectors, and optical accessories.

7.2 Absorption, Emission and Excitation Setups

Cary 219 and 500 Spectrophotometers: These instruments were used for low-resolution absorption spectra. Together these instruments cover a spectral range from 100 to 1000 nm. The instruments were controlled externally by using an IBM PC. The samples mounted on a cold finger of a closed cycle refrigerator could be inserted into the sample space. In this manner, these

instruments allowed for the recording of absorption as well as the transmission spectra of the sample in the temperature range from 10 to 300 K. For absorption spectra typical resolution of the Cary 219 and 500 instruments was better than ± 0.1 nm.

Excitation and Emission Setup: For better resolutions in shorter spectral range a dye laser based setup was used, Figure 7. In the excitation mode, its resolution is limited by the resolution of the laser, 0.03 cm^{-1}. In the emission mode, the resolution is limited by the resolution of the monochromator, 0.1 cm^{-1}. For the recording of the excitation spectra, the tunable laser beam was directed to the sample. The scattered laser light was filtered out and only the emission from the sample was focused onto a photomultiplier tube. In order to improve the signal to noise ratio, a phase sensitive detection using a light chopper and a lock-in amplifier was employed. The signal was normalized to the fluctuations in the laser power. The incident laser beam was split into two, the reference and the sample beams. The signal from the photomultiplier tube was divided by the power of the reference beam.

For the emission mode, the laser was fixed to the desired excitation wavelength and focused on the sample, Figure 8. The emission from the sample was focused onto the slit of the Spex 750 M monochromator. Appropriate filters were used to block the scattered laser light. The emission spectra were obtained by scanning the monochromator over the desired range.

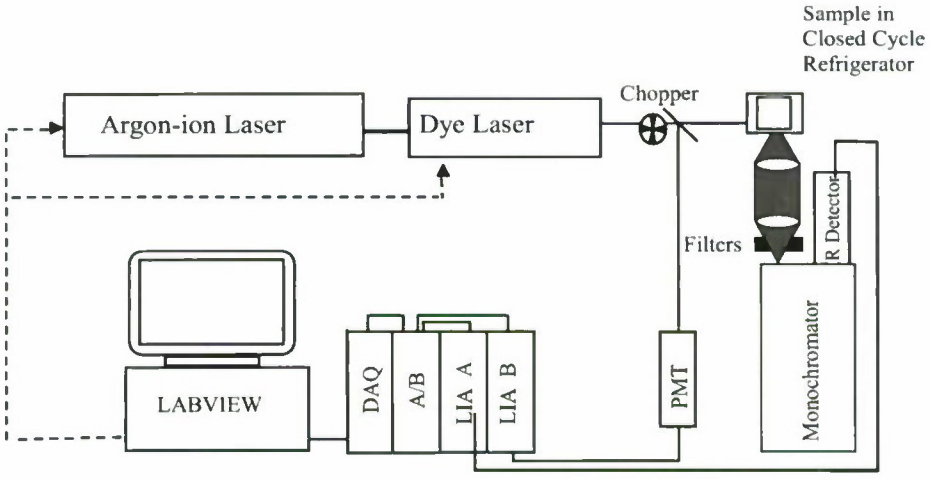

Figure 7. Sehematies of Laser Fluoreseenee Exeitation Setup

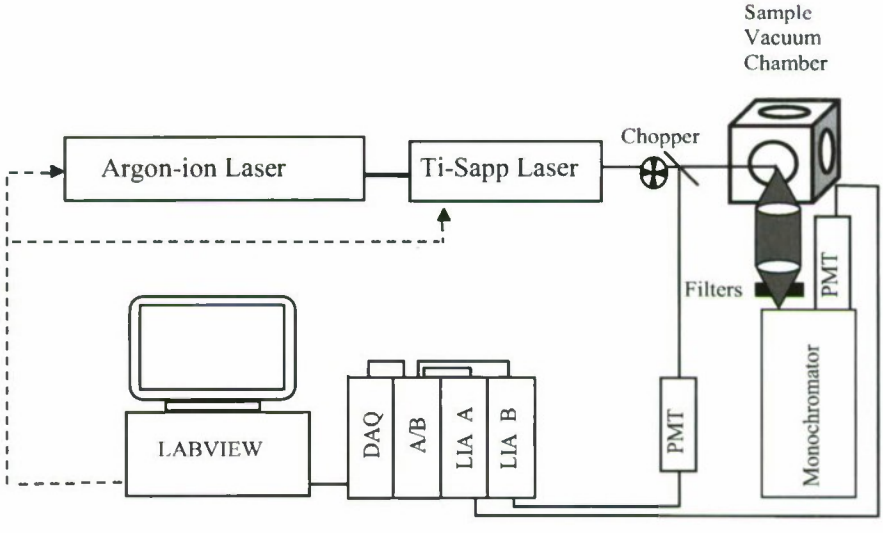

Figure 8. Schematics of emission setup

7.3 Pulsed Setup

This setup, Figure 9, was used for selective excitation and lifetime measurements. A Lambda Physik excimer laser Compex 102 was used for pumping the Lambda Physik LPD 3000 dye laser system. The output of excimer laser was in the form of 10 ns laser pulses with a maximum repetition rate of 100 Hz. The laser used a Xenon-Chlorine mixture that lases at 308 nm. It produces the maximum pulse energy of 200 mJ. This laser was controlled through trigger pulses from the dye laser. Each of these trigger pulses resulted in a laser pulse within 500 ns of the trigger. The dye laser had a GPIB interface and was controlled by computer through the software developed in LabView. By using the GPIB interface, the computer also controlled the trigger pulses that were generated from the dye laser. The detection system for lifetime measurements consisted of a photomultiplier tube (PMT), a boxcar integrator, and a preamplifier. The setup was completely synchronized by the trigger pulses generated from the dye laser, as shown in Figure 9(b). The laser beam was focused onto the sample. The emission was collected through a lens assembly and focused on the slit of a Spex 750M monochromator at 90 degrees with respect to the laser beam, Figure 9(a).

For the detection of the emission signal a Thorn EMI 9816B gated PMT was used. The PMT could be turned on and off by a gating circuit. The gated PMT was turned off during the laser pulse to prevent PMT overload due to the scattered laser radiation reaching it. This gating circuit changes the potential of the first dynode to be positive or negative with respect to the cathode. In this manner electrons from the cathode surface are repelled during the off time and amplified during the on time.

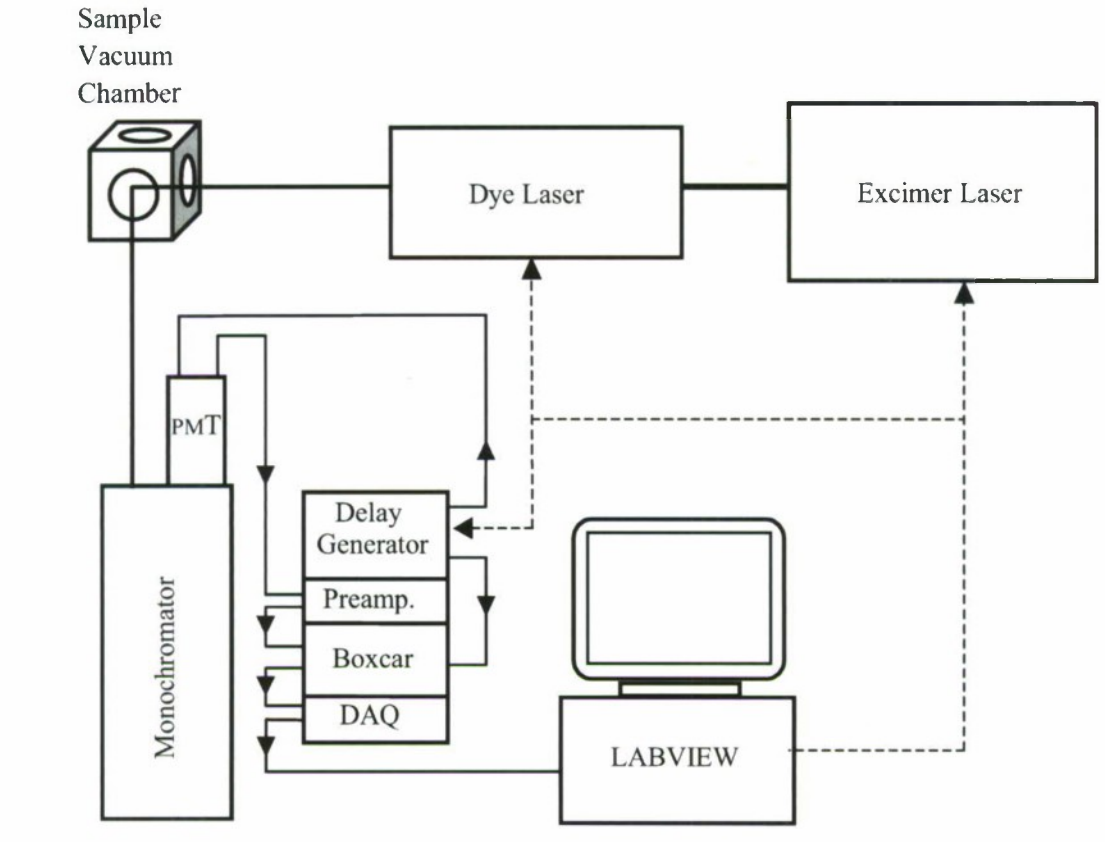

(a)

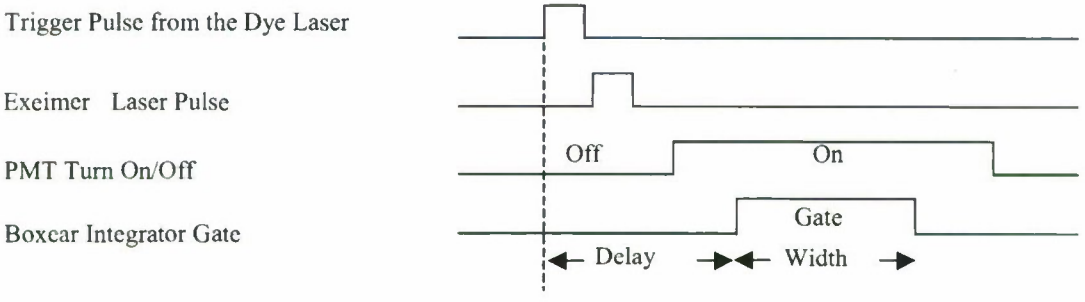

(b)

Figure 9. Experimental setup for lifetime, pulsed fluorescence, excitation and emission measurements. (a) Schematics of lifetime Measurement Setup; (b) Pulse train sequence for life time measurements.

The gating circuit had a limitation of 2 μs transition time between the on and off mode. The signal was amplified and recorded by a boxcar integrator. The gate delay and width for the boxcar integrator was varied as required for measuring the emission from the sample. For lifetime measurements, the gate was scanned over a time range of interest. In this manner emission from the sample was monitored following the sharp laser pulse.

7.4 Laser Cooling Setups

Figure 10 shows the laser cooling setup schematically and its photograph in the laboratory is shown in Figure 11. This setup was used for all laser cooling experiments reported here. The major components of this setup are: a Coherent 899-1 Ti-Dye laser that was employed as the cooling laser, a Coherent Sabre DBW 25/5 Ar-ion laser was used to pump the Ti-dye laser system. It had a maximum output power of 30 watts in the visible multi-line mode. The same laser was used as a source of excitation for some of the emission measurements.

The Coherent 899-1 laser system is a convertible laser system that can operate as a conventional ring dye laser or as a solid state ring laser by using Ti-sapphire as the gain medium. It is tunable from 375 to 750 nm in dye operations and from 0.68 to 1.025 microns as a solid state ring laser in Ti-sapphire mode. The Ti/dye laser was tuned to the desired wavelength by a three-plate bi-refrengent filter. In the energy range of interest, ~ 0.8 micron, maximum power output of this laser was in excess of 2.5 watts. The beam from the Ti- sapphire laser passes through the optical windows and impinges on the sample in the high vacuum chamber described below.

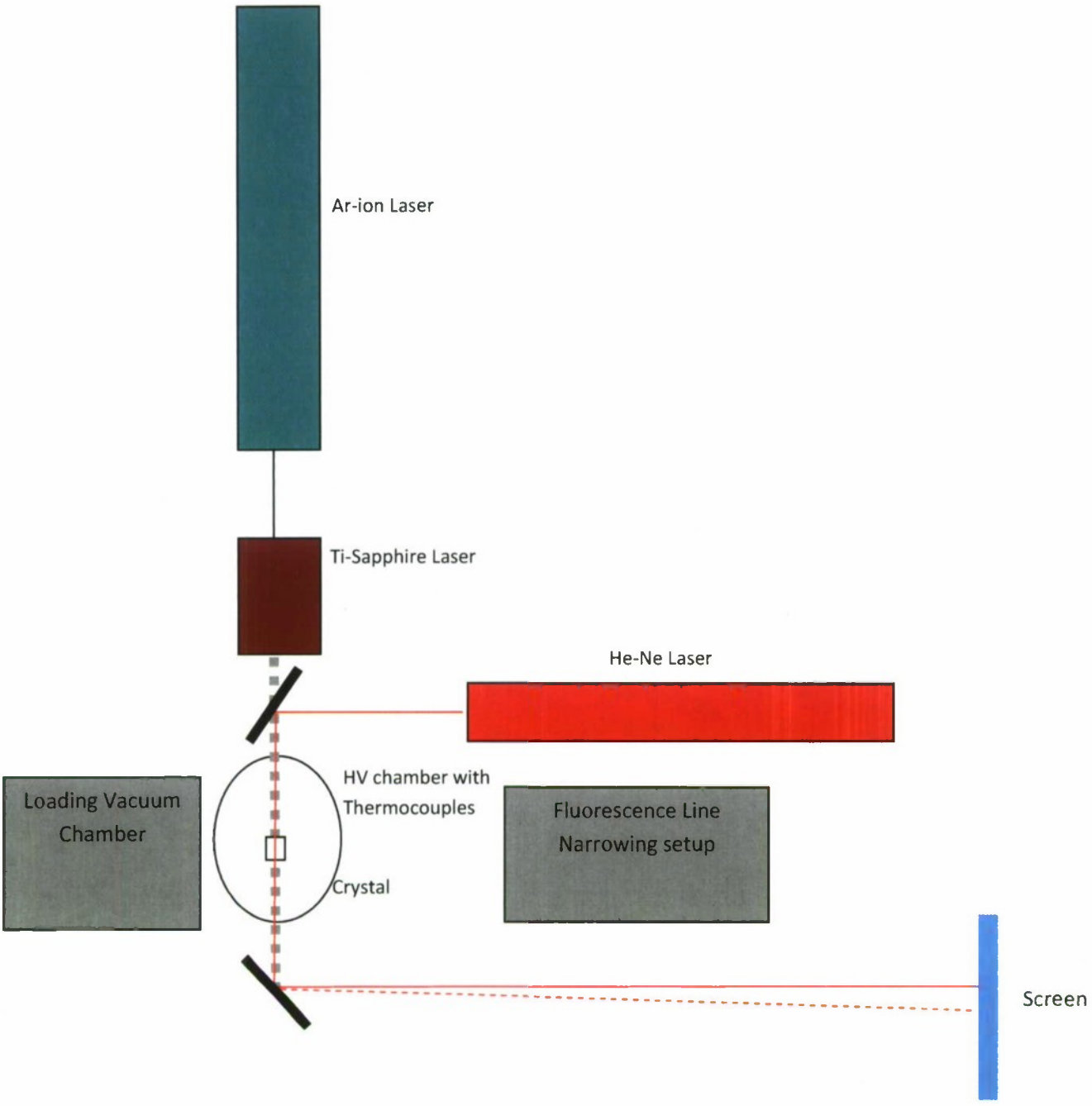

Figure 10. Sehematies of Laser Cooling Setup. Three setups ean be seen (i) Setup for Thermoeouple Deteetion, (ii) Photo-Thermal Defleetion and (iii) Emission Line Narrowing Setups

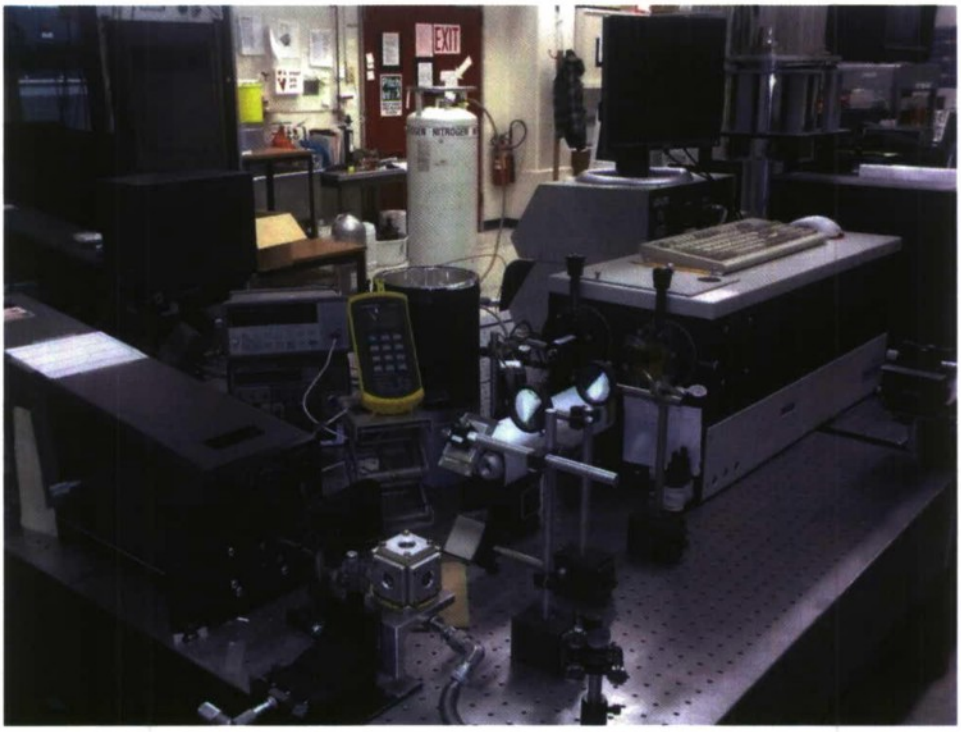

Figure 11. Laser cooling experimetal stations corresponding to the schematics of Figure 10. The sample in the chamber is kept at ~10^{-6} torr vacuum by the diffusiuon pump (not seen in the picture).

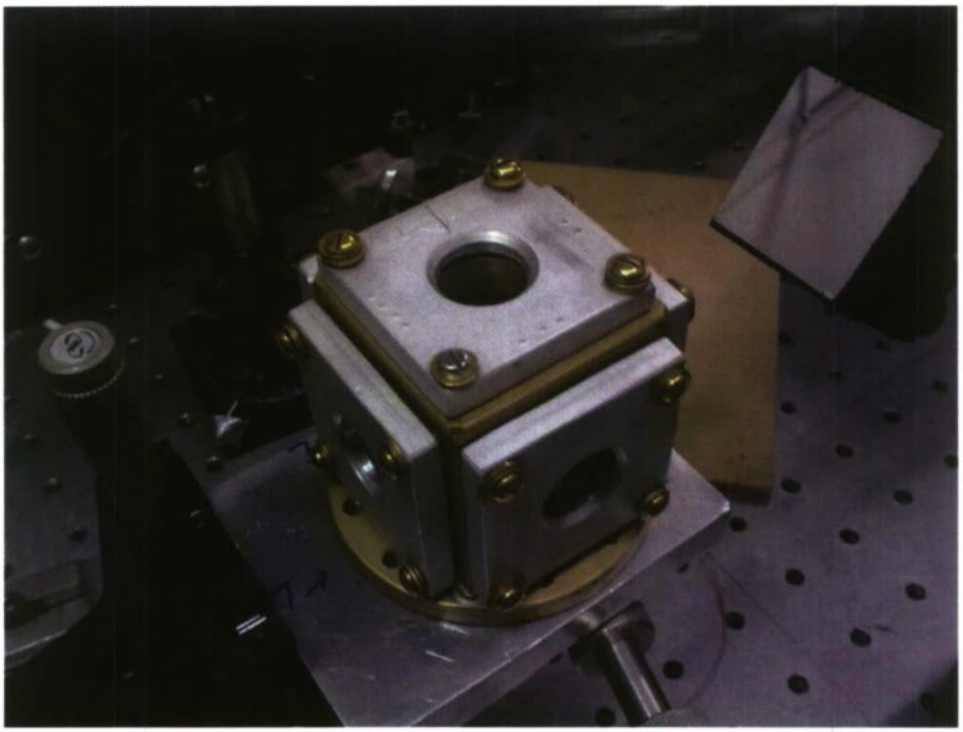

Figure 12. The sample vacuum chamber with IR calcium fluoride windows and thermocouple detectors attached to the base. The vacuum system on the left is not seen in the picture.

High Vacuum Chamber: The chamber is shown in Figure 12. For the three laser cooling experiments described below, four side optical windows were used. For the IR laser cooling a pair of calcium fluoride windows were used in the path of the incident laser. The top window was used for visual monitoring and the base window was used for introducing the sample. The chamber was mounted on a micro-controlled three axis optical platform. In this geometry it could be evacuated to a high vacuum ~10^{-6} torr using a diffusion pump. The sample was typically mounted on two glass micro-slides in a crossed position having the minimum point contact with the sample.

The cooling or heating of the sample was accomplished by the IR laser passing through the sample. At this stage, the change in crystal temperature can be monitored using one or more of the following techniques. These techniques monitor sample temperature independent of each other and therefore, we describe them separately.

7.4.1 Setup for Bulk Cooling Measurements

Measuring cooling by thermocouple detectors was the only method used for all the data presented here in this report. Two ultra-sensitive thermocouple junctions were employed to monitor any temperature changes upon laser irradiation of the sample. One probe monitored the change in crystal temperature while the other monitored the changes in the temperature of the chamber in the vicinity of the sample. The voltage signal of the two thermocouples was monitored on a dual channel Agilent pico-voltmeter, model 34420A. The difference signal of the two thermocouples was plotted as a function of time. This gave the difference in temperature of the sample and the chamber. The pico-voltmeter was controlled by a PC. To minimize the heat load on the sample by the thermocouple, a fine 0.001 inch diameter, Omega Company's Chromel–Alumel thermocouple was used.

7.4.2 Photo-Thermal Deflection Setup

In this case, an additional probe beam, He-Ne laser, passes collinearly with the cooling beam through the crystal and monitors its temperature. A change in temperature causes a change in the refractive index of the crystal that is measured by the deflection of the probe Helium-Neon laser. Cooling and heating will give rise to deflection of the probe beam in opposite directions. The magnitude of deflection can be related to the cooling efficiency. He-Ne is a localized probe that measures the changes in the same volume that has been cooled; therefore, it can always overestimate cooling. This setup has been tested for some transparent samples but has not been tried with our hygroscopic samples that deteriorate at the surface very quickly. This causes serious scattering of the beam.

7.4.3 Setup for Fluorescence Line Narrowing Measurements

These measurements monitor the crystal temperature by measuring the narrowing of rare earth spectral lines. It is built around a grating spectrograph and sensors in the IR and visible regions of the spectrum. Again this has not been tried for the measurements performed on our samples. This is a suitable technique for temperature differentials that are substantially larger than ours, usually tens of degrees Kelvin or more.

7.5 Cryogenic Facilities

Most of the optical spectroscopic experiments on the above described set ups were performed at or around room temperatures, 300 K. For other optical characterization experiments the temperature of the samples was varied from 15 to 300 K.

For absorption, excitation and emission measurements the sample temperature was typically varied from 7 to 300 K. This was possible by using an APD Industries, Displex DE-202 closed cycle refrigerator. The samples were mounted on a copper holder attached to the cold finger of the closed cycle refrigerator. To provide good thermal conduction an indium seal was placed in between the contacts. The stabilization in temperature was achieved by a resistive heater element situated next to the sample. The heater element was controlled by a temperature controller, Scientific Instruments model 9620. The temperature controller provided a stable temperature to ± 0.5 K of the actual temperature with an accuracy of ± 0.2 K. The temperature of the sample was monitored using a silicon diode that had an accuracy of ± 0.5 K for the temperature range 0 to 100 K and ± 1 % of the measured value in the 100 to 475 K range. It should be noted that these were not the cooling experiments where better accuracy and stability of temperature are needed.

8. Results on Optical and Laser Cooling Studies on Er-Based Materials

In this section we present, mainly, two types of results for Er-based solids that we have used in our studies, $Cs_2NaYCl_6:Er^{3+}$, $KPb_2Cl_5:Er^{3+}$ and ZBLAN:Er^{3+}. The results cover data on laser cooling and associated spectroscopic investigations. First, experimental data on absorption and emission spectra at room temperature and lower temperatures were analyzed to extract the general information about the cooling characteristics. A comparison of $KPb_2Cl_5:Er^{3+}$ and ZBLAN:Er^{3+} optical spectra and cooling characteristics is made with the cubic host $Cs_2NaYCl_6:Er^{3+}$.

As described earlier, for optical refrigeration we performed only the thermocouple measurements to detect cooling/heating of these samples. This method has the advantage that it detects cooling of the bulk. Secondly, in all of our experiments, the cooling laser had the single pass geometry; no attempts were made nor were necessary for our strongly absorbing crystals to construct a multiple-pass cavity. The photo-thermal deflection experiments provide a complimentary method of detection, but by itself their data can be less conclusive of cooling. These experiments also require very high quality surface polishing. That has been demanding for our hygroscopic $Cs_2NaYCl_6:Er^{3+}$ crystals. We therefore gave preference to thermocouple detection. However, in the light of our success in laser cooling these efforts of obtaining complimentary data will not be postponed for long.

The organization in the following subsections is as follows. First, the optical and laser cooling data and its analysis are presented for $Cs_2NaYCl_6:Er^{3+}$ system. Then the results of the same experiments performed on a $KPb_2Cl_5:Er^{3+}$ crystal will be presented. Under the same

conditions and with the maximum available cooling laser power this crystal did not show any cooling. Rather, we registered a net heating of the sample. The third system, ZBLAN glass doped with erbium, is in the process of being polished and prepared for the cooling experiments to be performed soon. Therefore, we will present only optical spectroscopy data on this system to draw some general conclusions about the suitability of this system for laser refrigeration.

8.1 Optical and Laser Cooling Studies in $Cs_2NaYCl_6:Er^{3+}$

Optical spectroscopy, emission and absorption studies were very essential as the cooling transitions are very weak. These spectra are sometimes not even possible to record and in the range of laser cooling which is always done by pumping the low energy wing of the absorption this is particularly true. We therefore give the full spectra in emission and absorption in all details. Although the signal may be very weak due to the additional difficulty of having very poor detectors in the 0.8 micron region where laser cooling has been most effectively and conclusively observed we have observed all of these transitions.

8.1.1 Absorption and Emission Studies

The spectra for the absorption from the ground state to three lowest lying IR multiplets; $^4I_{15/2}$ - $^4I_{13/2}$, $^4I_{15/2}$ - $^4I_{11/2}$, and $^4I_{15/2}$ - $^4I_{9/2}$ of Er in Cs_2NaYCl_6 are shown in Figure 13. These three states are directly or indirectly involved in the laser refrigeration reported so far in Er. The spectra were taken on Cary 500 at room temperature. The nominal concentration of Er in this sample was 80% as allowed by the formula. The $^4I_{15/2}$ - $^4I_{13/2}$ transition was the strongest and required a different absorbance scale and therefore has been superimposed on the spectra for our

concentrated sample. Otherwise, the weaker transitions, particularly $^4I_{15/2}$ - $^4I_{9/2}$, would not be detectable.

The absorption strengths of these transitions as calculated from the full crystal field wave functions for these states (Section 5.4) are also given in the units of 10^{-8} (Debye)^2. In this spectrum the absorption of $^4I_{15/2}$ - $^4I_{9/2}$ is exaggerated as a change of detector and a filter in the IR is necessary at the position where the peak of this absorption occurs. This gives rise to a vertical line in the spectrum as the baseline changes the slope at this point, Figure 13. This all gives rise to an artificial signal that is not part of $^4I_{15/2}$ - $^4I_{9/2}$ absorption. Therefore, it is a very weak

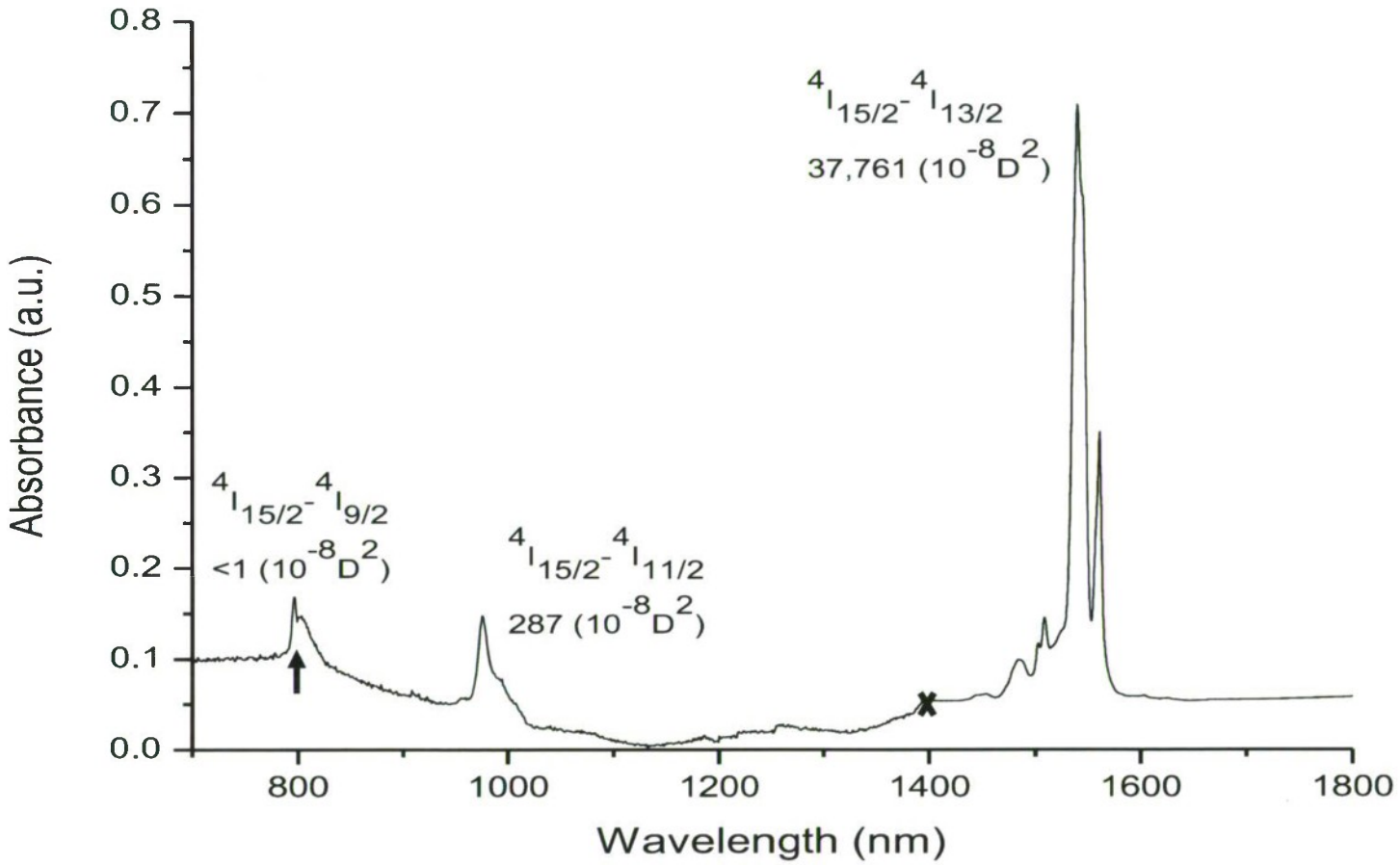

Figure 13. Absorption Spectrum of $Cs_2NaYCl_6:Er^{3+}$ at room temperature. The crystal had a nominal concentration of 80% Er allowed by the chemical formula.

transition to compare from this spectrum. The calculated and observed absorption strengths for $^4I_{13/2}$ and $^4I_{11/2}$ transitions follow the correct ratios for their intensities.

(i) $^4I_{15/2}$ - $^4I_{9/2}$ Transition: The absorption spectrum of the $^4I_{15/2}$ - $^4I_{9/2}$ transition is shown at high resolution in Figure 14. It should be noted that $^4I_{15/2}$ - $^4I_{9/2}$ is the weakest transition. It is forbidden by the total orbital angular momentum selection rules ($\Delta J=3$, $\Delta L=0$); it is electric dipole forbidden as it is a transition between states that are within the f^n configuration; and, finally, the cubic crystal field may put some restrictions due to symmetry selection rules. It becomes allowed just by a small admixture of other states such as $^4I_{13/2}$, by crystal field and other higher order perturbations. Therefore, observing $^4I_{15/2}$ - $^4I_{9/2}$ was always a challenge, especially at room temperature. This intensity is further distributed throughout the vibronic bands. Hence, we see a faint tail of absorption in the room temperature spectra extending towards low energy range. The sharp peak ~800 nm is also the result of the change of filter as described in the case of Figure 13 above. Beyond 850 nm the absorption signal is indistinguishable from the noise. There is small but significant absorption beyond 820 nm. Attempts to take a better spectrum in the 820-880 nm region are in progress as this is very crucial for the cooling experiments and the interpretation of the results to be presented in the following sections. The center of mean absorption is ~805 nm.

The high resolution emission spectrum at room temperature for the $^4I_{15/2}$ - $^4I_{9/2}$ transition is given in Figure 15. It covers the same energy range as the absorption of Figure 14 for comparison. The mean fluorescence wavelength from this spectrum is ~815 nm. This is significant as it is related to the efficiency of cooling.

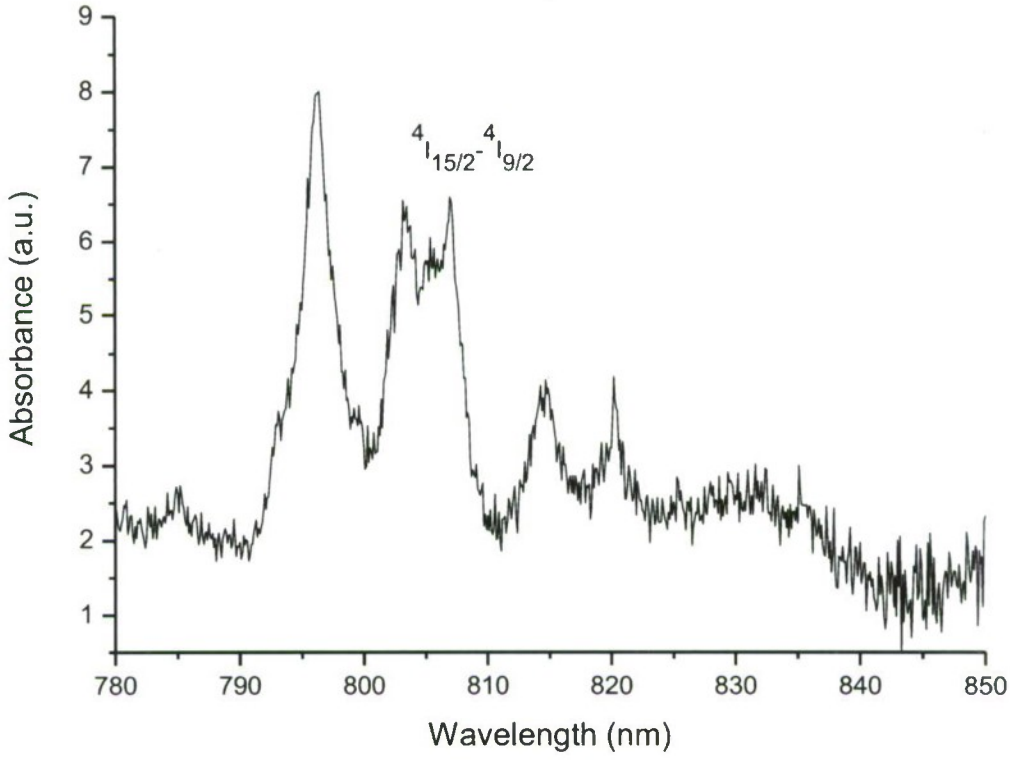

Figure 14. Room temperature absorption of $^4I_{15/2}$-$^4I_{9/2}$ in $Cs_2NaYCl_6:Er^{3+}$

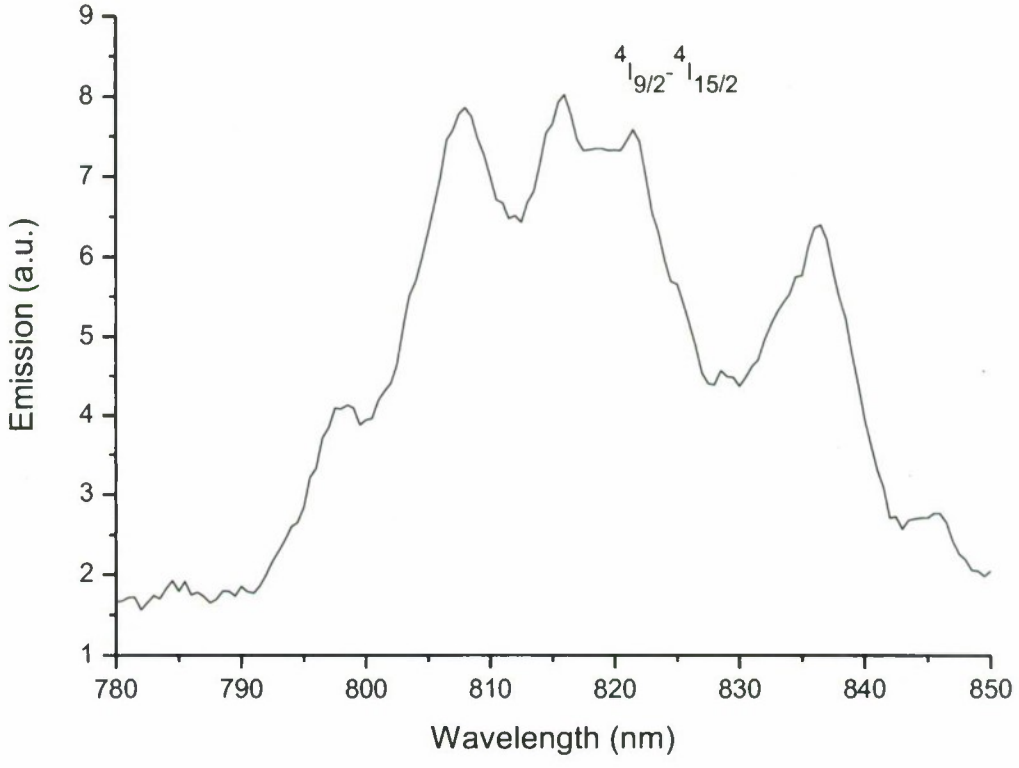

Figure 15. Room temperature emission of $^4I_{15/2}$-$^4I_{9/2}$ in $Cs_2NaYCl_6:Er^{3+}$

(ii) $^4I_{15/2}$ - $^4I_{11/2}$ Transition: In Figure 16 the absorption spectrum of the $^4I_{15/2}$ - $^4I_{11/2}$ transition is shown at high resolution. $^4I_{15/2}$ - $^4I_{11/2}$ is a hypersensitive transition; it is slightly allowed by the total orbital angular momentum seleetion rules ($\Delta J=2$, $\Delta L=0$ *and* $\Delta S=0$). Other seleetion rules are the same as in the $^4I_{15/2}$ - $^4I_{9/2}$ transition; it is eleetrie dipole forbidden as it is a transition between states that are within the f^n eonfiguration. It beeomes allowed by just a small admixture of other states sueh as $^4I_{13/2}$, by erystal field and other higher order perturbations. An 11% admixture of $^4I_{13/2}$ in $^4I_{11/2}$ state wavefunetions will result in the observed intensity of this transition as seen in the speetra.

The emission speetrum for this transition is given in Figure 17 with the mean emission wavelength of ~ 992 nm. The speetrum is slightly red shifted eompared to the absorption spectrum. The bad signal to noise ratio is due to the poor response of our detector, a Thorn-EMI 965 Photo multiplier Tube in this ease.

(iii) $^4I_{15/2}$ - $^4I_{13/2}$ Transition: This is the strongest transition of Er^{3+}. For many reasons that we will diseuss later, it is the most promising transition for laser eooling. The optieal strength of this transition eomes from the faet that this transition is magnetie dipole allowed and spin allowed; $\Delta J=1$, $\Delta L=0$ and $\Delta S=0$.

The absorption and emission speetra are given in Figures 18 and 19. The strong absorption verifies the highest calculated oscillator strength, ~38000 (10^{-8} D^2) for this transition.

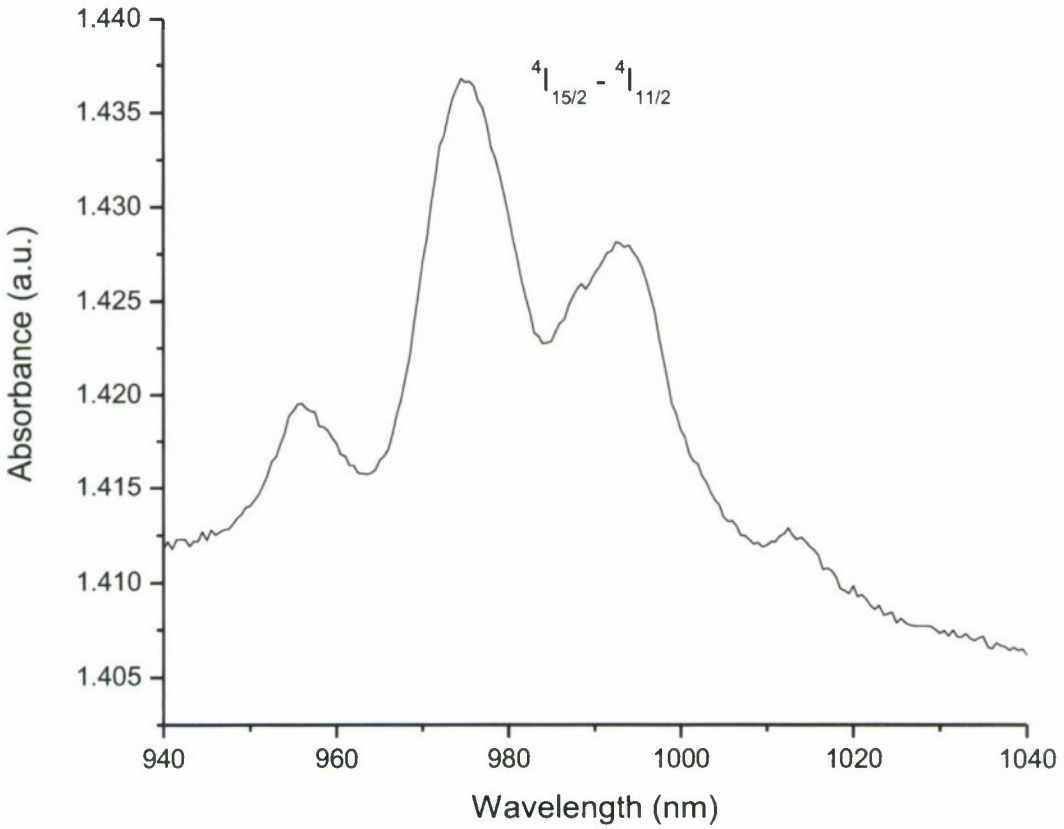

Figure 16. Room temperature absorption of $^4I_{15/2}$-$^4I_{11/2}$ in $Cs_2NaYCl_6:Er^{3+}$

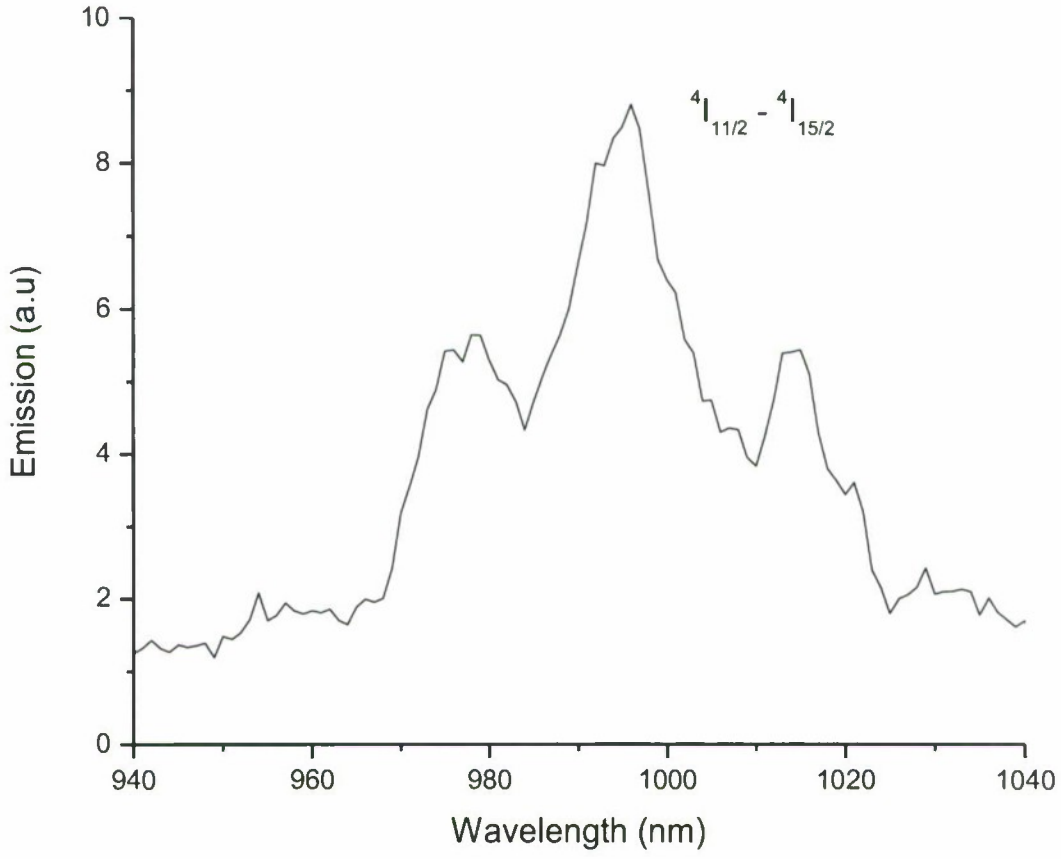

Figure 17. Room temperature emission of $^4I_{15/2}$-$^4I_{11/2}$ in $Cs_2NaYCl_6:Er^{3+}$

8.1.2 Laser Cooling Studies

As of the date of this report, bulk cooling by more than 6 degrees Kelvin has been observed by pumping the $^4I_{15/2}$ - $^4I_{9/2}$ transition in $Cs_2NaYCl_6:Er^3$. Laser cooling has only been tried in the $^4I_{15/2}$ - $^4I_{9/2}$ transition of Er. The main reason for it was the availability of lasers in our laboratory. A Ti-Sapphire laser working in the middle IR region was useful for these experiments. In our lab it is pumped by an Ar-ion laser. In the following we describe the optimizations performed on different components of the cooling setup Figure10 to achieve laser-cooling in our systems.

(i) Cooling Laser: As $^4I_{15/2}$ - $^4I_{9/2}$ is the weakest transition; there were serious demands on the pump laser as well as the detection techniques. The power output of the cooling Ti-Sapphire laser was maximized to more than 2.5 Watts in continuous working mode in the 808-900nm range. This required the optimum performance from the pump Ar-ion laser; a multi-line output of 30 watts in the blue green region with TEM00 mode was necessary for the desired IR power. High pump power required a very careful operation of the laser with optimum cooling of the Ti-Sapphire crystal to save it from heat damage from the high power pump laser. For the maximum cooling reported here exposures as long as 30 minutes were tried with the maximum IR power of 2.25 watts in the 802-885nm range.

(ii) Crystals: The main advantage of our crystal was its high concentration of erbium ~ 80% allowed by the formula. This could have been increased to 100% but was a limit set by the availability of good optical quality single crystals of a reasonable size; in our case rectangular bi-prism of 3mm x 3mm x 8mm. Two great advantages of our crystal were as follows:

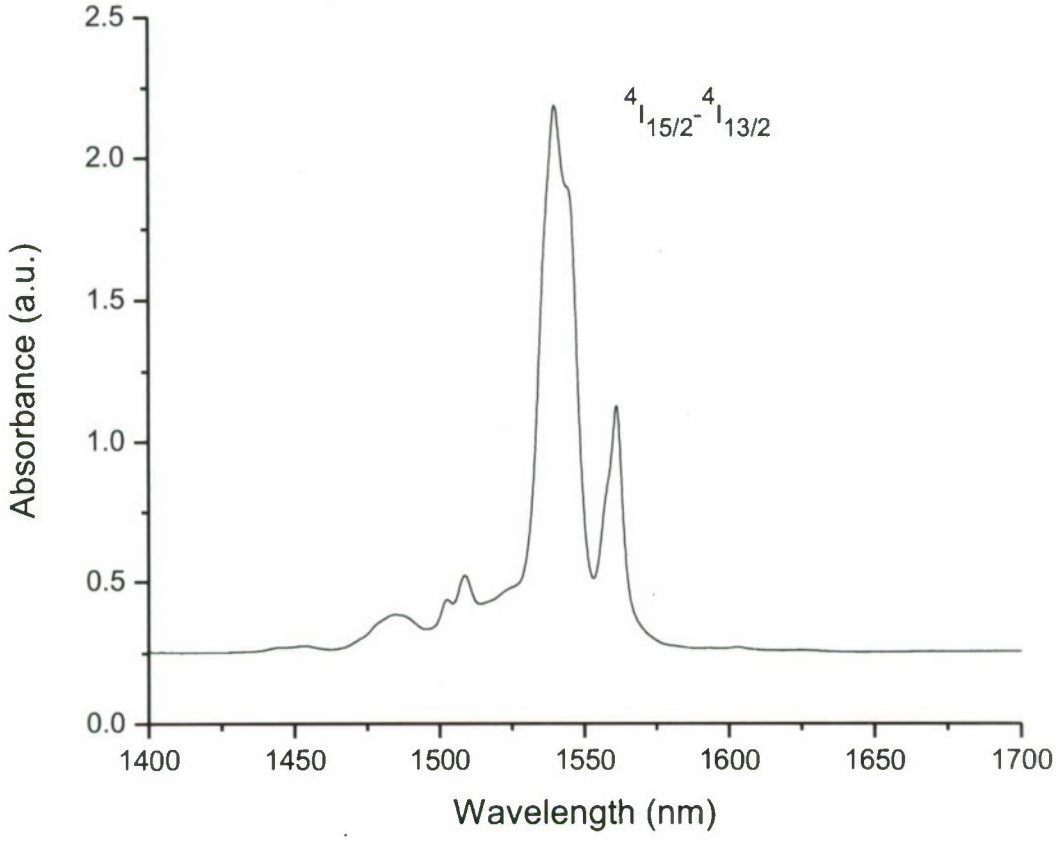

Figure 18. Room temperature absorption of $^4I_{15/2}$-$^4I_{13/2}$ in $Cs_2NaYCl_6:Er^{3+}$

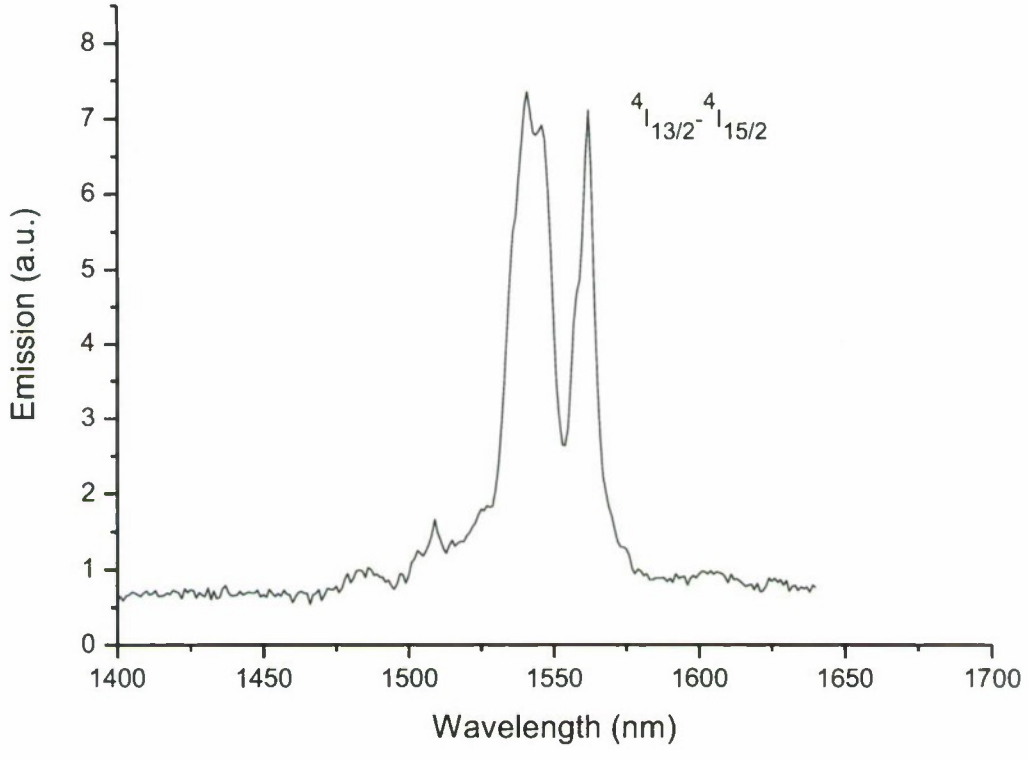

Figure 19. Room temperature emission of $^4I_{15/2}$-$^4I_{13/2}$ in $Cs_2NaYCl_6:Er^{3+}$

- The high concentration of erbium, 80%, made the effective optical length much larger without increasing the bulk heat load of the crystal.

- In addition, no multiple passes were needed to absorb the laser efficiently as is normally practiced to achieve lower cooling temperatures.

$Cs_2NaYCl_6:Er^{3+}$ crystals are highly hygroscopic, i.e., they absorb water from the atmosphere very readily. Therefore, several glove boxes for cutting, polishing and loading of crystals as described earlier were needed. Even then, the crystal surfaces were far from optical quality and deteriorated further with time. Thus, repetitive polishing was necessary during a series of experiments, or at the time of loading the crystals or just after opening the chamber for any reason.

(iii) Thermocouple Detectors: To minimize any conductive thermal contact, the crystals were mounted on crossed micro-slides held on a plexi-glass platform. Two identical thermocouples, 0.001'' diameter chromel-alumel, Omega CHAL-001were mounted on the side of the crystal; one to measure the temperature of the chamber and the other was in contact with the crystal to measure its temperature changes during and after the irradiation. Both thermocouples were shielded from the incident laser beam during the experiment and only the crystal was directly exposed to the beam. In order to cancel out any geometric effect of the positioning of the two thermocouple sensors, the experiments were repeated with their positions interchanged. The same optical cooling/heating effects were observed in both cases. The occurrence of any such spurious effects were further investigated and eliminated by studying several dummy samples on the same setup under the same conditions. Such experiments invariably resulted in heating those samples as expected. The second junctions of the two

thermocouples were kept at a constant temperature in an ice bath. The thermocouple measuring the crystal temperature was held with a micro-drop of glue and in some cases without glue. The glue did not cause any appreciable heat load.

(iv) Cooling Data Acquisition and Analysis: The voltages across thermocouple junctions were recorded using an Agilent pico-voltmeter, model 34420A.

As the incident beam results in the heating of the chamber the difference of the voltages from two sensors was taken as the signal of net cooling/heating of the sample. In this case, the sample was irradiated with a laser at 870 nm and a power of 1.6 watts for 7 minutes. This is the wavelength where the maximum cooling was observed. The data is plotted in Figure 20 (a) (solid line) as a function of time starting from 30 seconds after switching the incident laser off. After this time interval, all short-term effects such as sensor cooling, chamber cooling, etc., are greatly reduced.

The wavelength dependence of cooling was measured by the same thermocouple detection systems from 802 nm to 880 nm; it gives ~832 mm as the reversal wavelength. Below this wavelength heating and above it net cooling was observed. The data was analyzed by using two exponentials, one for the reference thermocouple and the other for the reference thermocouple as shown with the dashed dotted line and dashed lines respectively.

The maximum cooling from Figure 20 (a) is ~1.5 K whereas we observed a temperature change of more than 6 K from the room temperature, when the sample was irradiated with a power of 2.27 Watts for 30 minutes, Figure 20 (b). The thick solid line is the temperature difference between the sample and the chamber. The collection time starts 10 seconds after the

laser beam has been turned off. The thick dashed line is the initial fit to the data that gives ~6 K cooling below the environment. The sample was irradiated for 30 minutes with 2.3 watts of IR cooling laser power. These data are being analyzed at this time. We believe a temperature lowering of more than 6 K can be extracted from an improved analysis.

(v) Discussion

It was clear that we needed high cw-pumping powers for extended times to observe better cooling by pumping the 0.8 micron transition. Cooling in this transition, as is generally the case, is achieved by pumping in the low energy wings of the absorption band. Therefore, extended time and high power exposures are needed for any detectable cooling of the bulk. This requirement is hardly unusual. Even for the best Yb based systems more than 10 watts cooling laser powers and exposures of several hours are not uncommon [9]. Attempt to achieve lower temperatures of cooling by optimizing other parameters are in progress.

The cooling we observed is significantly more than what was observed in previous works on erbium based materials; an order of magnitude better than observed by Fernandez, ~ 0.3 K for $^4I_{15/2}$ - $^4I_{9/2}$ transition in $KPb_2Cl_5:Er^{3+}$ and two orders of magnitude better than Condon et. al. in ZBLAN:Er^{3+} while optically pumping $^4I_{15/2}$ - $^4I_{13/2}$ transition. As we will discuss later, the latter comparison is not even fair as the transition of interest in that case had four to five orders of magnitude stronger absorption strength and therefore should exhibit very different behavior than for the cooling in $^4I_{15/2}$ - $^4I_{9/2}$. Here we limit ourselves to the 0.8 micron $^4I_{15/2}$ - $^4I_{9/2}$ transition.

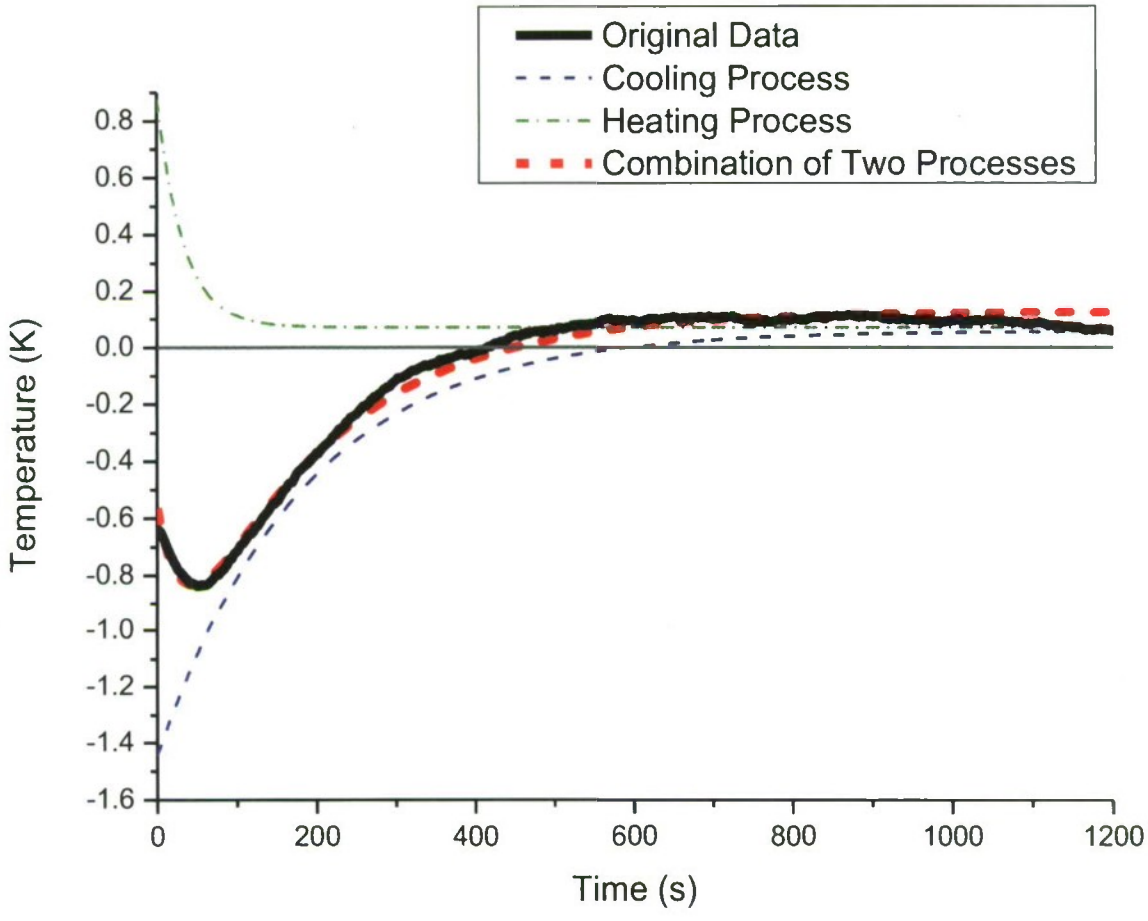

Figure 20. (a) Laser cooling result and fitting for $Cs_2NaYCl_6:Er^{3+}$ in the $^4I_{15/2}$-$^4I_{9/2}$ transition. The thick solid line is the temperature difference between the sample and the chamber. The zero time starts 30 seconds after the laser beam has been turned off. Dotted lines are the behavior of the crystal and the chamber represented by two exponentials. The thick dashed line is the fit to the data.

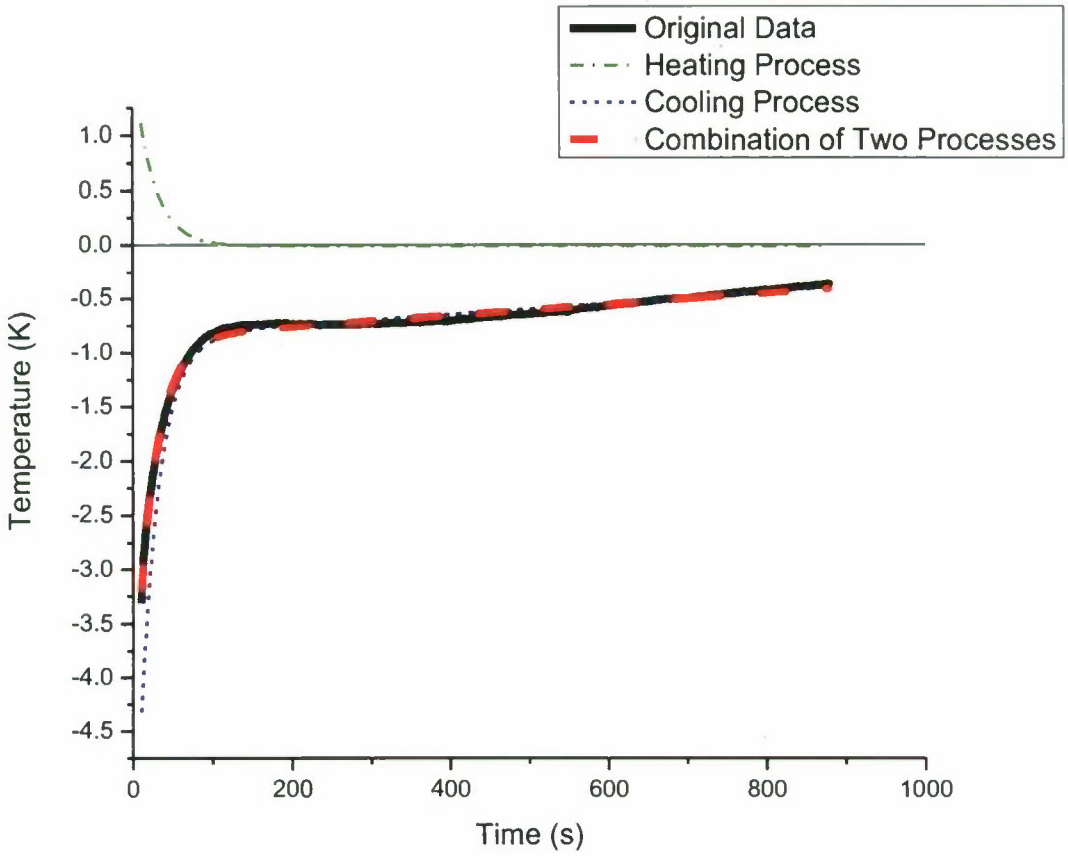

Figure 20. (b) Maximum laser cooling: experimental result and initial fitting for $Cs_2NaYCl_6:Er^{3+}$ in the $^4I_{15/2}$-$^4I_{9/2}$transition. The thick solid line is the temperature difference between the sample and the chamber. The collection time starts 10 seconds after the laser beam has been turned off. The thick dashed line is the initial fit to the data that gives ~6 K cooling below the environment. The sample was irradiated for 30 minutes with 2.3 watts of IR cooling laser power.

Fernandez et. al [23] reported cooling in the same transition as ours but in a different host: $KPb_2Cl_5:Er^{3+}$. Their confirmatory experiments for cooling were based on thermal deflection spectroscopy, whereas the absolute measurement of crystal temperature was done by an IR camera. Such measurements were disputed by other workers. Condon et. al. [24] tried to study cooling in the same crystal, $KPb_2Cl_5:Er^{3+}$ using the same transition ${}^4I_{15/2}$ - ${}^4I_{9/2}$. Their detection technique employed thermocouples to measure the temperature changes in the bulk. Condon et. al. did not find any bulk cooling although their setup was capable of detecting temperature changes of better than 0.01 K. Therefore, Condon et. al. concluded that there was no cooling. They argued that photo-thermal deflection signals as observed by Fernandez could have resulted from some other spurious effects of transient population in the excited states causing changes in the refractive index. They also questioned IR camera results that were supposed to show some very localized cooling in the first place according to Fernandez et. al. As we see for temperature difference measurements neither Fernandez et. al. employed thermocouples nor Condon et. al. tried to observe photo-thermal deflection although both had comparable concentrations of Er in their good optical quality crystals.

Our crystals discussed here are different but our temperature measurements use the same technique as used by Condon et. al. Our observation of cooling does neither prove nor totally disprove the results disputed in the case of 0.8 micron transition in $KPb_2Cl_5:Er^{3+}$. We will discuss our experiments on that crystal in a later section where we discuss $KPb_2Cl_5:Er^{3+}$ system in detail. At this stage, we discuss the prospects of cooling in $Cs_2NaYCl_6:Er^{3+}$using other low lying transitions of Er^{3+}.

The $^4I_{15/2}$ - $^4I_{11/2}$ transition, according to the optical studies presented in the earlier section deserves some attention. It has higher absorption strength than the $^4I_{15/2}$ - $^4I_{9/2}$ transition. The $^4I_{11/2}$ state is known to facilitate optical upconversion processes. Therefore, any significant population in this state was feared to give heating contributions rather than cooling. There is no fundamental reason for this to happen. Therefore, cooling in $^4I_{15/2}$ - $^4I_{11/2}$ transition will be tried at a later stage when our Ti-sapphire laser can be switched to work in this region of the spectrum. It is not a bad transition to try for cooling. The most important transition of our interest is $^4I_{15/2}$ - $^4I_{13/2}$ that will be discussed next.

8.1.3 Prospects for 1.5 Micron Cooling

Orders of magnitude better cooling results using the weakest transition, $^4I_{11/2}$ - $^4I_{9/2}$ are very encouraging for trying our system for 1.5 micron cooling using the $^4I_{15/2}$ - $^4I_{13/2}$ transition. As can be seen in Figure 19, the mean fluorescence wavelength is slightly blue shifted in the room temperature spectrum, clearly suggesting that its potential for cooling is high. With our high concentration system, the more promising transition at 1.5 microns, $^4I_{15/2}$ - $^4I_{13/2}$ has many advantages over the $^4I_{15/2}$ - $^4I_{9/2}$ transition:

- This transition requires laser photons of half as much energy as the 0.8 micron transition for extracting the lattice energy. Therefore, the first law efficiency of cooling, equation (1), is doubled.
- The $^4I_{15/2}$ - $^4I_{13/2}$ transition is 10^4-10^5 times stronger absorption in comparison, so optical pumping should be easier in this case.

- Diode lasers for pumping the $^4I_{15/2}$ - $^4I_{13/2}$ transition are commercially available. These lasers are less expensive, less bulky, robust and easy to operate in comparison to the Ti-Sapphire pump used for the $^4I_{15/2}$ - $^4I_{9/2}$ cooling.

- One potential loss mechanism of cooling power for $^4I_{9/2}$ state is it's depopulation by non-radiative relaxation to the nearby $^4I_{11/2}$ state, thus creating multiple phonons and heating the crystal. In contrast, the $^4I_{13/2}$ state lies ~6000 cm^{-1} above the ground $^4I_{15/2}$ state. Therefore, at room temperature, more than twenty phonons will be needed to depopulate it by radiation-less-multi- phonon relaxations. This is a better transition for cooling.

At this stage, a comparison of this transition with the Yb-doped ZBLANP is fair where record temperatures of cooling, 208 K, were observed. The transition used in that case was also a magnetic dipole allowed transition with comparable absorption strength as our $^4I_{15/2}$ - $^4I_{13/2}$ transition of erbium. However, it is the total absorption of the laser radiation that matters for cooling. Therefore, in their low concentration samples, exposures of several hours with more than 10 watts of laser power were needed by Epstein [9]. The absorption of laser power was further enhanced by forming a cavity with reflective mirrors at the end thus creating a multiple-pass of the beam that consequently resulted in cooling their samples to such low temperatures. We believe that our systems with high concentrations of erbium would potentially have many advantages for cooling.

8.2 Optical and Laser Cooling Studies of $KPb_2Cl_5:Er^{3+}$ and ZBLAN

Most of the conditions for the optical studies of the $KPb_2Cl_5:Er^{3+}$ and ZBLAN:Er^{3+} systems were the same therefore we group them together in this section. The only difference being that ZBLAN:Er^{3+} has not been tried for the cooling in our laboratory as yet.

$KPb_2Cl_5:Er^{3+}$ is the only crystal where optical cooling has been demonstrated by pumping in its two IR transitions, $^4I_{15/2}$ - $^4I_{9/2}$ (0.8 micron) and $^4I_{15/2}$ - $^4I_{13/2}$ (1.5 micron). Therefore, after our crystal $Cs_2NaYCl_6:Er^{3+}$, this was the first crystal used by us to compare and confirm cooling/heating results. ZBLAN:Er^{3+} is a glassy system and therefore it does not have any restrictions of crystal symmetry selection rules. It is a well-known host for laser cooling also due to its attractive vibrational characteristics.

8.2.1 Absorption and Emission Studies

The overall absorption spectrum of the three IR transitions for $KPb_2Cl_5:Er^{3+}$ and ZBLAN:Er^{3+} at room temperature is shown in Figures 21 and 22. The spectra were taken for unpolarized light and with no specific orientation of the $KPb_2Cl_5:Er^{3+}$ crystal. Apart from the difference of the poor signal to noise ratio, the spectra in Figures 21 and 22, have all general features as the elpasolite crystal, $Cs_2NaYCl_6:Er^{3+}$, Figure 13. As far as the intensity ratios of different transitions, their energies, and crystal field spreads are concerned, the two systems, $KPb_2Cl_5:Er^{3+}$ and ZBLAN:Er^{3+} are nearly identical to each other and not in any qualitative way different from $Cs_2NaYCl_6:Er^{3+}$. This observation makes two strong points worth noting about cubic systems:

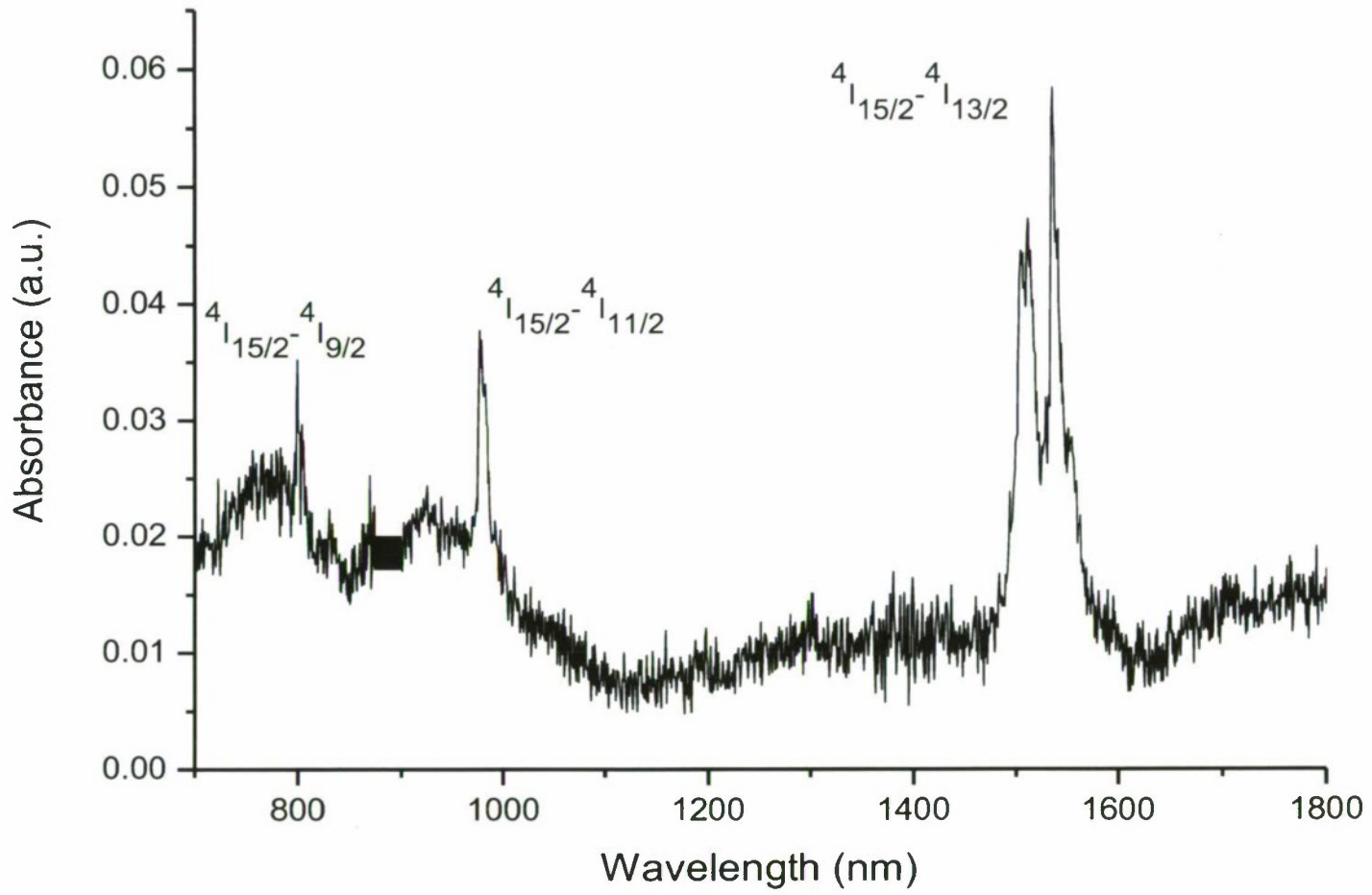

Figure 21. Room temperature absorption spectrum of $KPb_2Cl_5:Er^{3+}$

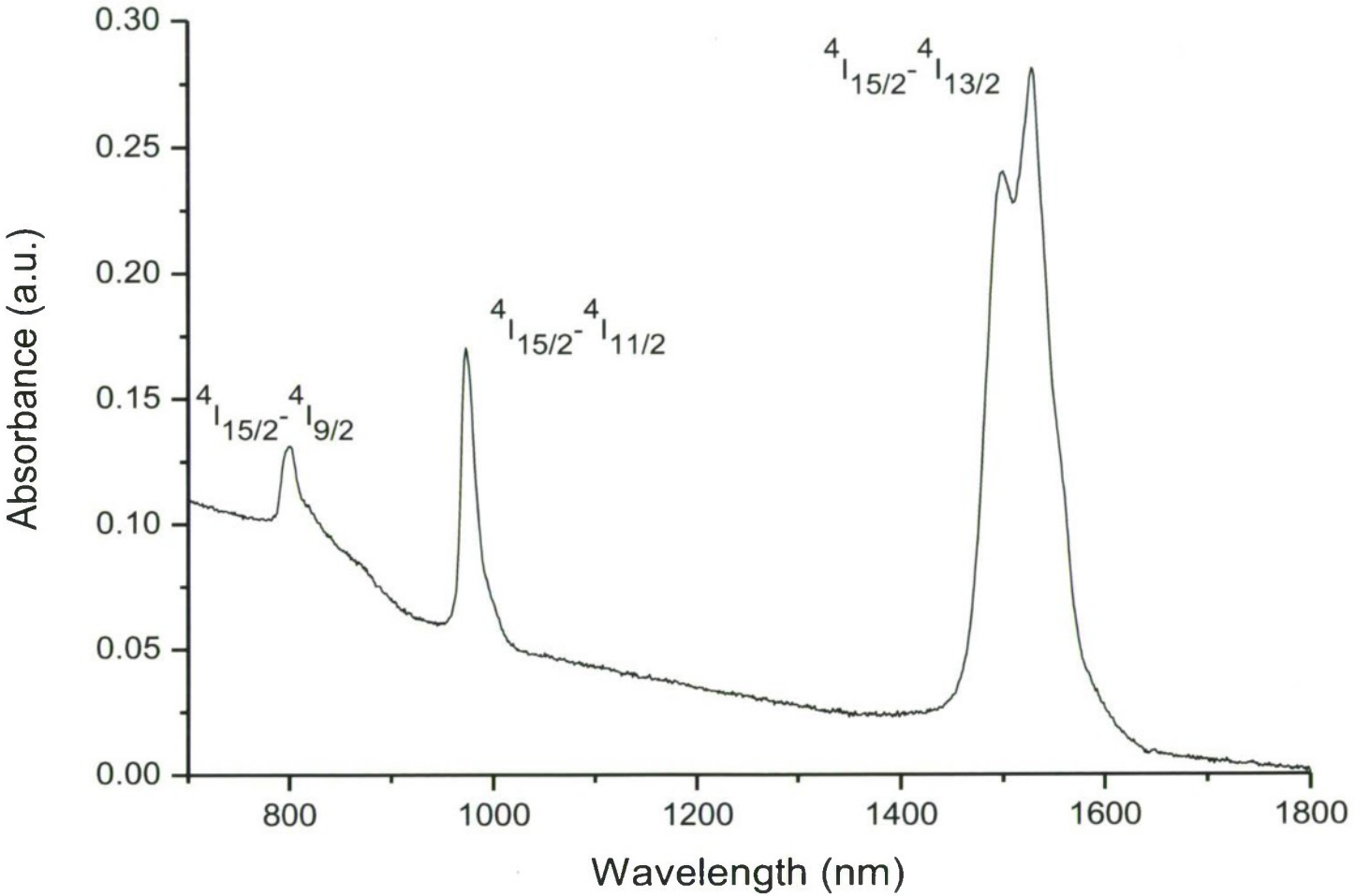

Figure 22. Room temperature absorption spectrum of ZBLAN:Er^{3+}

- First, this similarity suggests that we can use the calculations that are good for cubic system, such as for calculating crystal field energies and relative absorption strengths as a guideline for non-cubic systems or even glasses. This is very important for a general understanding of the processes involved in cooling.

- Second, the cubic systems are not as forbidding for optical transitions as one would expect on the basis of only cubic selection rules. Mixing of L-S states by any perturbations such as the crystal field give magnetic dipole as well as electric dipole intensities to otherwise forbidden transitions. All these details should be worked out by calculations before making any easy but potentially erroneous conclusions.

(i) $^4I_{15/2}$ - $^4I_{9/2}$ Transition: The room temperature absorption and emission with high resolution are given in Figures 23 and 24 for $KPb_2Cl_5:Er^{3+}$. For $KPb_2Cl_5:Er^{3+}$ the emission has a mean fluorescence wavelength of ~855 nm and is considerably red-shifted from the absorption that peaks at ~802 nm. In the case of ZBLAN:Er^{3+} Figures 25 and 26, this shift is slightly smaller ~850 nm. This is attesting to the fact that these systems should show less potential for cooling as compared to $Cs_2NaYCl_6:Er^{3+}$. This will be discussed in the later section. The sharpness of the peak in absorption around 800 nm is a spurious effect as described for $Cs_2NaYCl_6:Er^{3+}$ above, an experimental limitation.

(ii) $^4I_{15/2}$ - $^4I_{11/2}$ Transition: The room temperature absorption and emission spectra are given in Figures 27 and 28 and Figures 29 and 30, for comparison in the two systems. Once again, for both systems the overall emission is red shifted and therefore, this transition may not be a good candidate for efficient cooling as compared to the $^4I_{15/2}$ - $^4I_{9/2}$ transition in either of

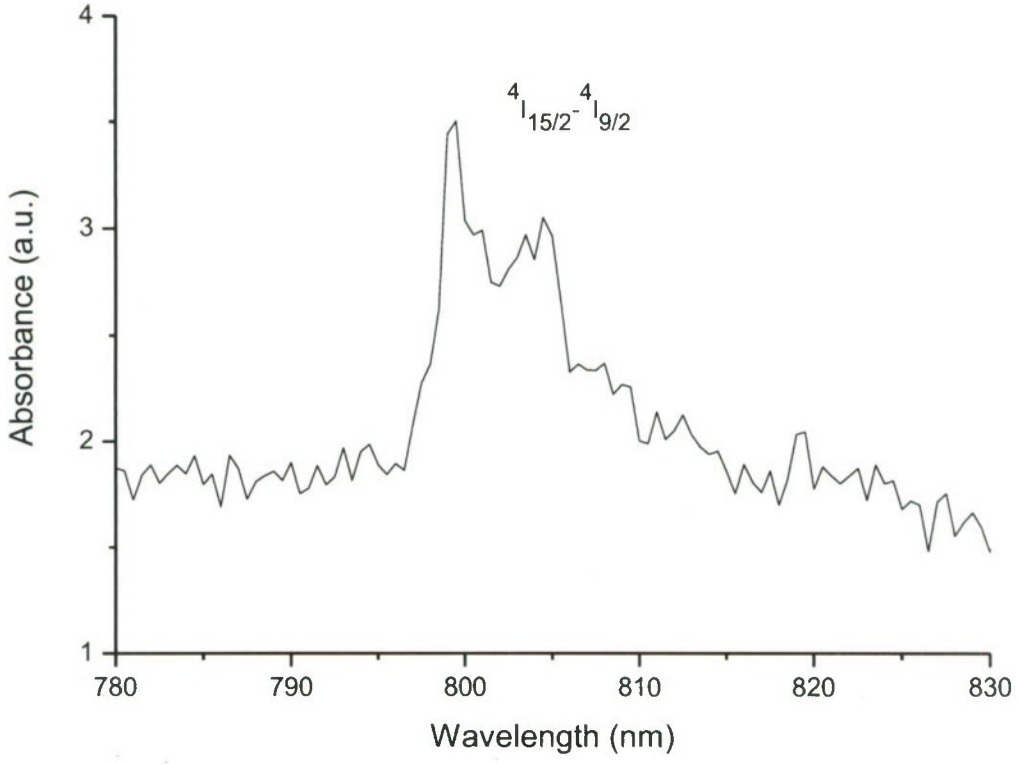

Figure 23. Room temperature absorption of $^4I_{15/2}$-$^4I_{9/2}$ in $KPb_2Cl_5:Er^{3+}$

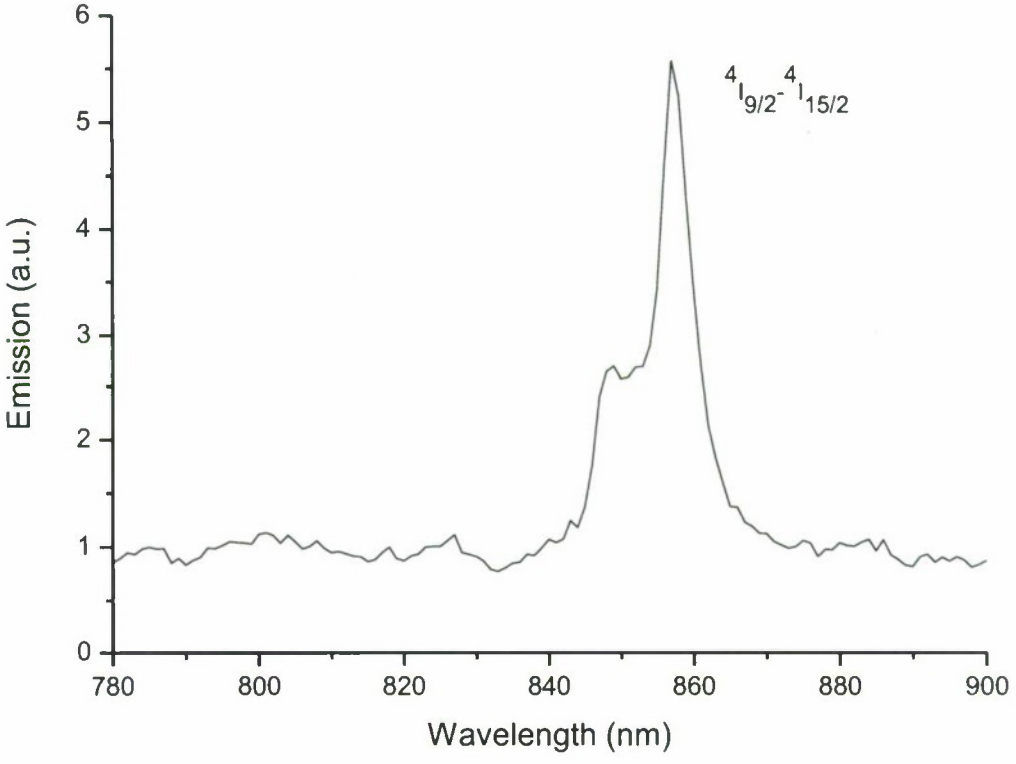

Figure 24. Room temperature emission of $^4I_{15/2}$-$^4I_{9/2}$ in $KPb_2Cl_5:Er^{3+}$

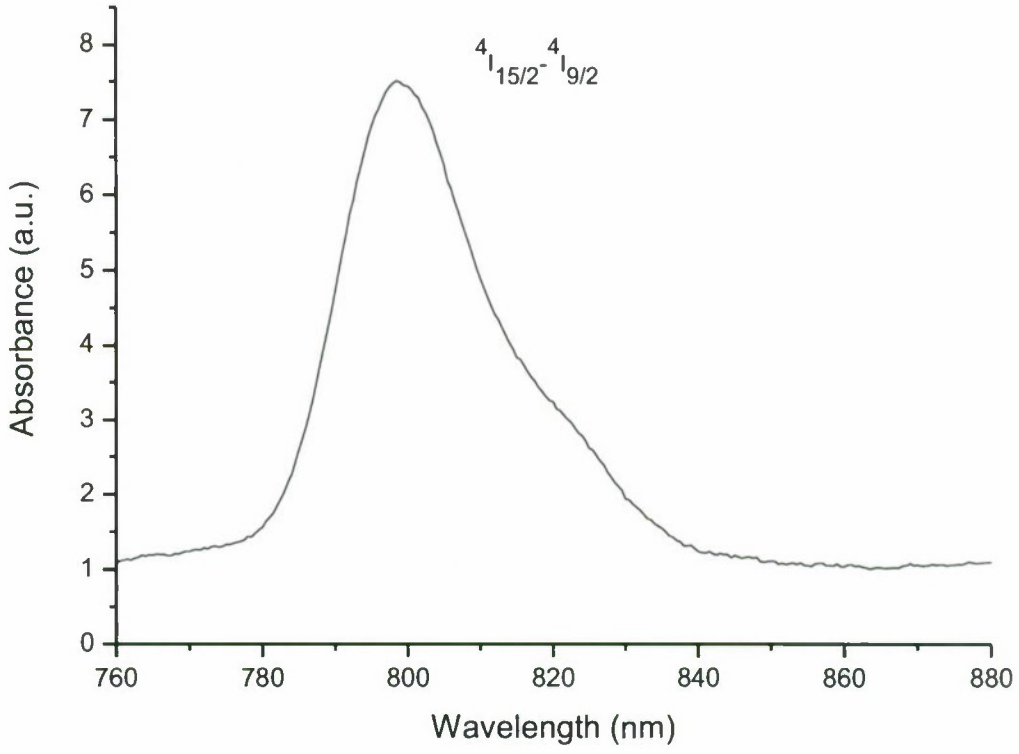

Figure 25. Room temperature absorption of $^4I_{15/2}$-$^4I_{9/2}$ in ZBLAN:Er^{3+}

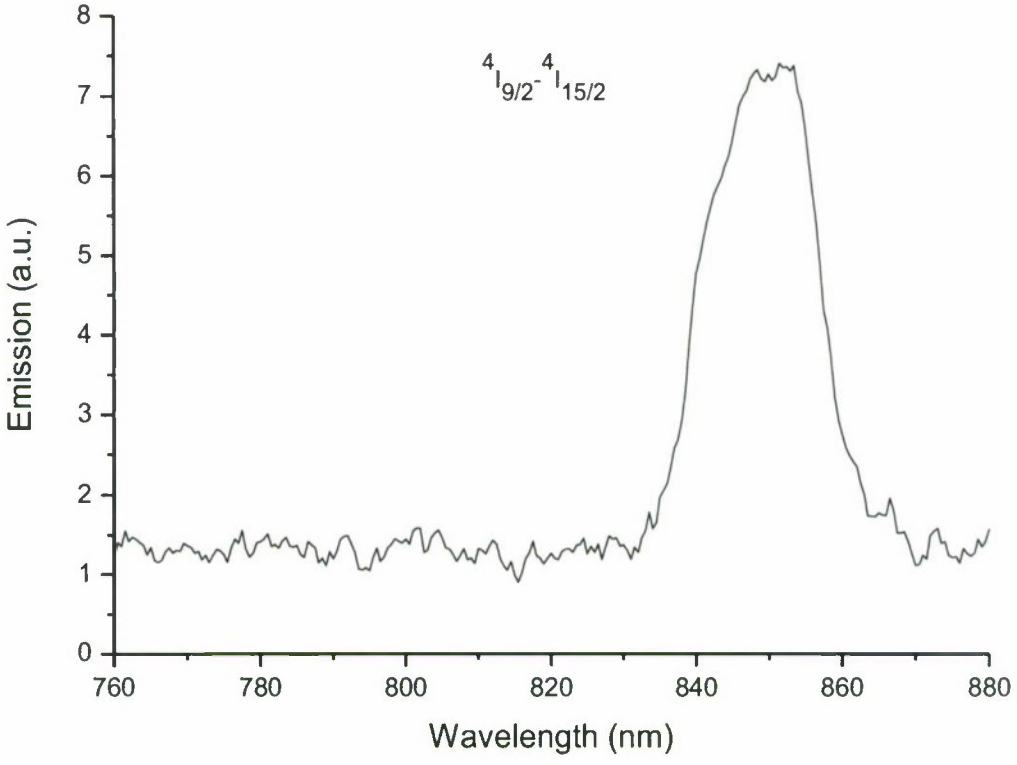

Figure 26. Room temperature emission of $^4I_{15/2}$-$^4I_{9/2}$ in ZBLAN:Er^{3+}

these solids, $KPb_2Cl_5:Er^{3+}$ and ZBLAN:Er^{3+}. It should be noted that the relative absorption strength of this transition in $KPb_2Cl_5:Er^{3+}$ and ZBLAN:Er^{3+} is as high as for the $Cs_2NaYCl_6:Er^{3+}$system. This gives preference to $Cs_2NaYCl_6:Er^{3+}$ as a system to be tried for cooling.

(iii) $^4I_{15/2}$ - $^4I_{13/2}$ Transition: The absorption and emission spectra for the two systems are shown in Figures 31 and 32 and Figures 33 and 34. For this transition there is a marked difference between $KPb_2Cl_5:Er^{3+}$ Figure 32 and $Cs_2NaYCl_6:Er^{3+}$ Figure 19 or ZBLAN:Er^{3+}, Figure 34. In $KPb_2Cl_5:Er^{3+}$ there is clearly one extra strong emission band at room temperature. This has serious implications for the cooling in this transition as discussed later.

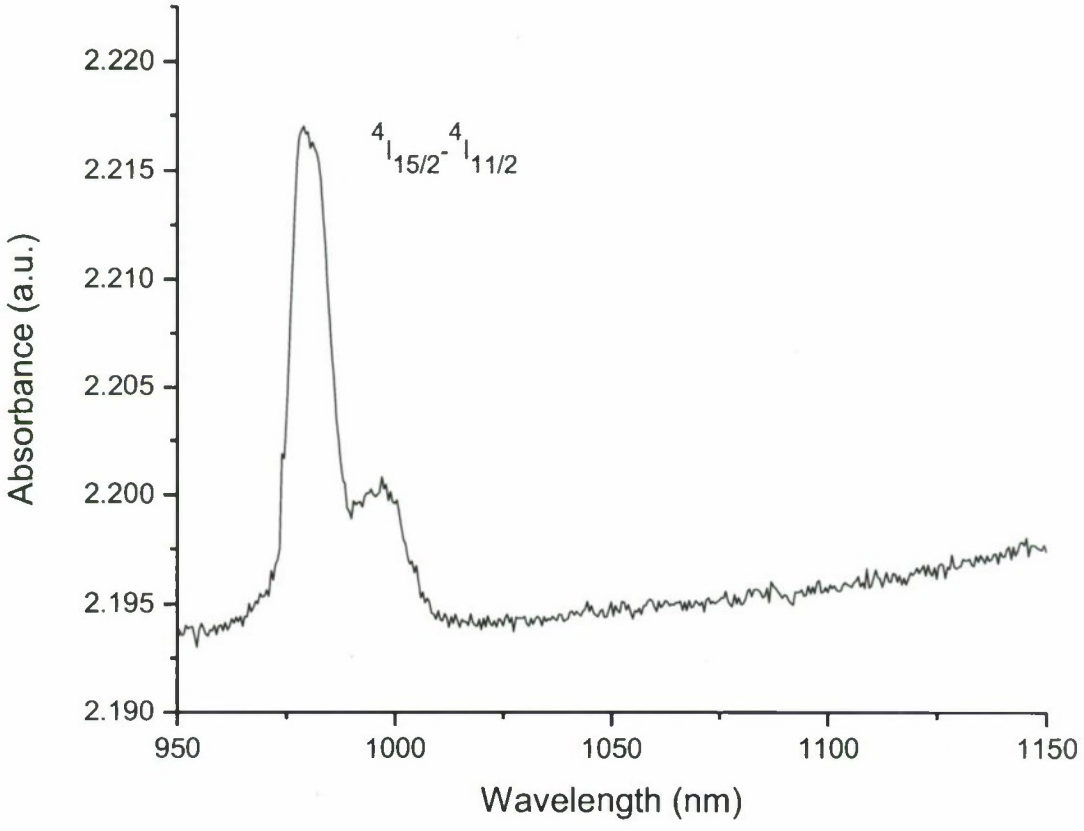

Figure 27. Room temperature absorption of $^4I_{15/2}$-$^4I_{11/2}$ in $KPb_2Cl_5:Er^{3+}$

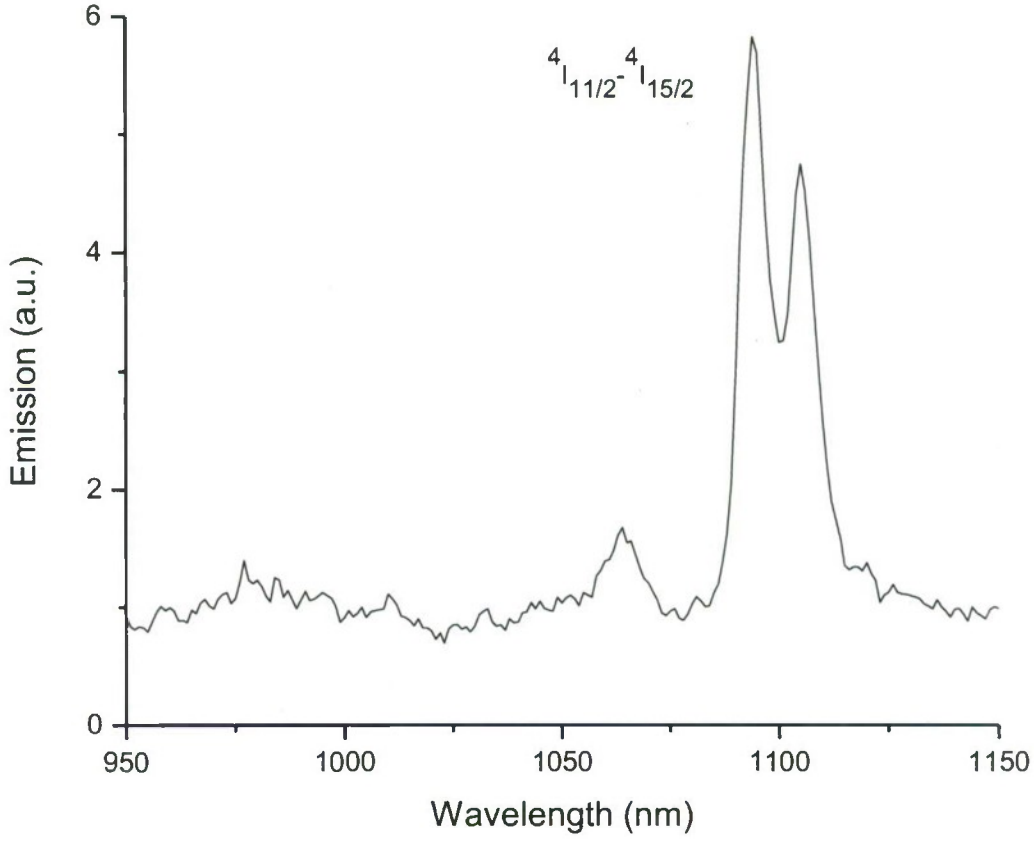

Figure 28. Room temperature emission of $^4I_{15/2}$-$^4I_{11/2}$ in $KPb_2Cl_5:Er^{3+}$

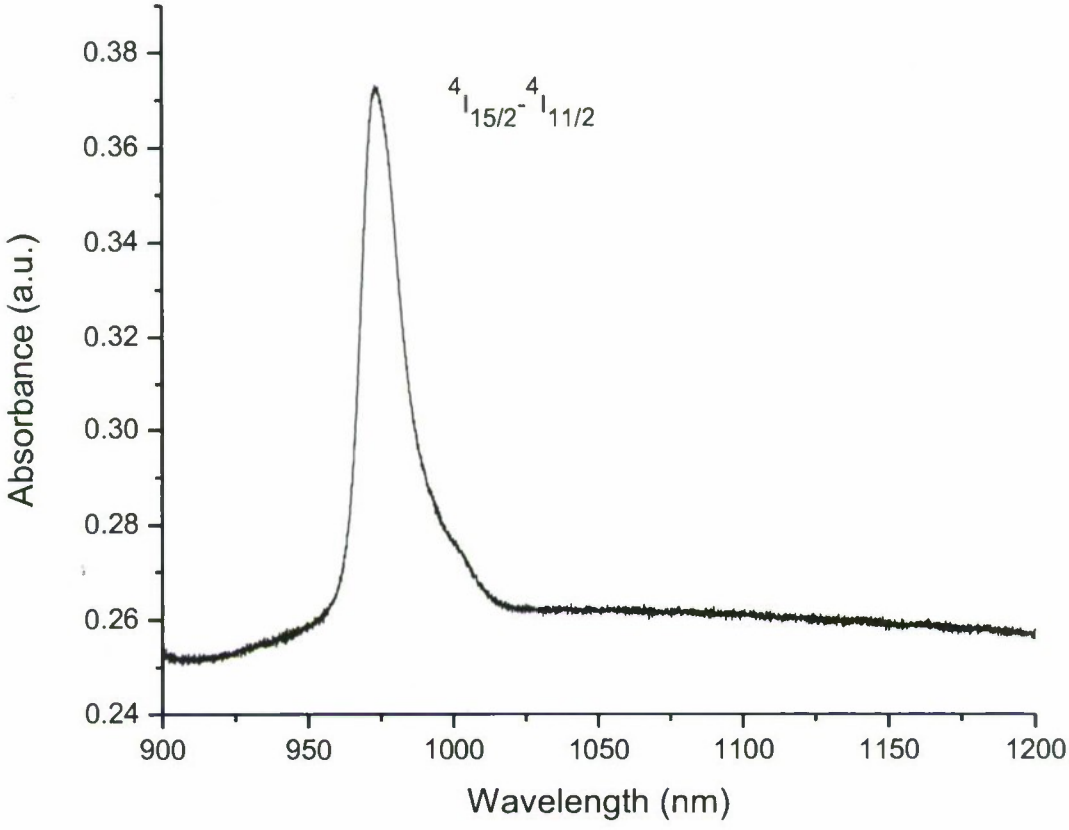

Figure 29. Room temperature absorption of $^4I_{15/2}$-$^4I_{11/2}$ in ZBLAN:Er^{3+}

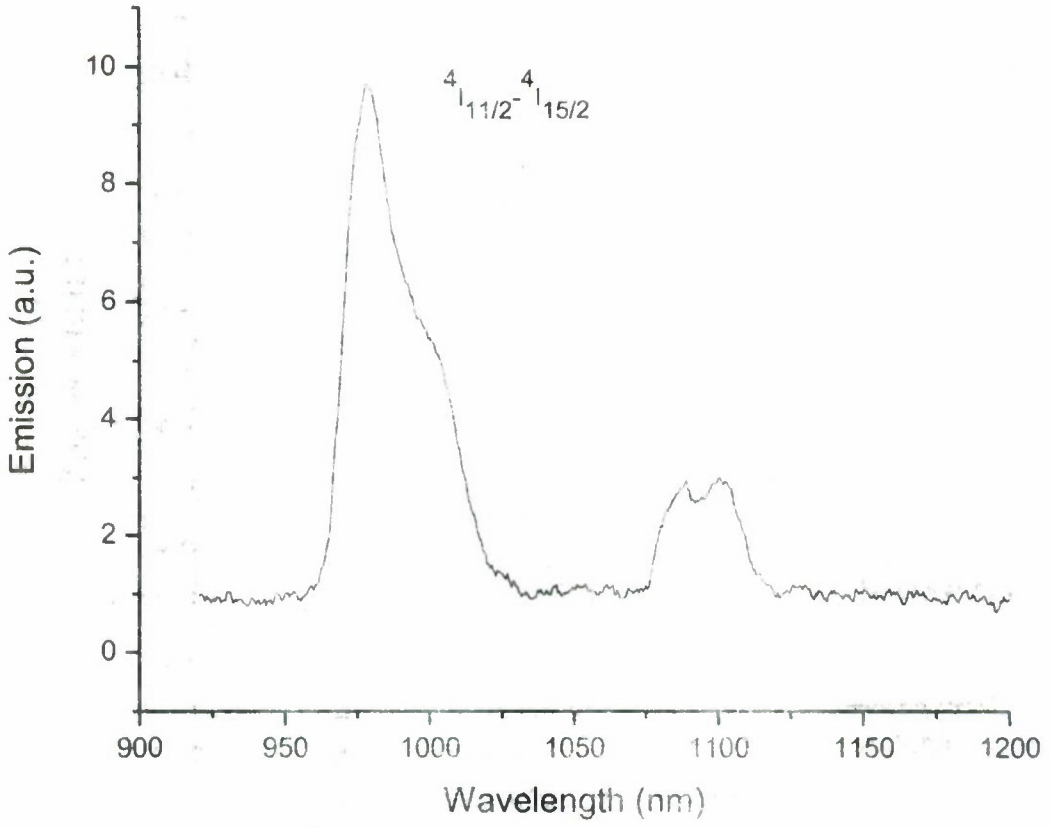

Figure 30. Room temperature emission of $^4I_{15/2}$-$^4I_{11/2}$ in ZBLAN:Er^{3+}

8.2.2 Laser Cooling Studies of $KPb_2Cl_5:Er^{3+}$

$^4I_{15/2}$ - $^4I_{9/2}$ 0.8 micron Cooling: Cooling was tried for the $^4I_{15/2}$ - $^4I_{9/2}$ transition at 0.8 microns. Our crystals had a nominal concentration of ~1% Er by formula of $KPb_2Cl_5:Er^{3+}$. The $KPb_2Cl_5:Er^{3+}$ crystal was smaller in dimensions as compared to the $Cs_2NaYCl_6:Er^{3+}$ crystal and therefore a smaller thermal load. Cooling was tried on the same setup as described in the case of $Cs_2NaYCl_6:Er^{3+}$ and under similar conditions. The input laser power was over 1.8 Watts. Under these conditions the crystal showed an overall heating rather than cooling.

Our observation of heating for this crystal system does not mean that we can conclusively discard Fernandez's results of observing localized cooling by Photo-Thermal deflection Spectroscopy. The cooling was so localized as to be in the center of a focused spot of the incident laser intensity; these authors observed cooling in a small area of a few pixels square on their IR camera screen. We could not have detected such a change by our thermocouples that were attached to the side of our $KPb_2Cl_5:Er^{3+}$ crystal even if it was there. Better photo-thermal deflection experiments are needed before making any conclusions.

Another solid host that we would try for cooling is ZBLAN glass. This, in its vibrational properties, is very close to Fernandez's system. The absorption and emission overlap in this system is again poorer than $Cs_2NaYCl_6:Er^{3+}$, our system discussed above. Therefore we would expect the cooling/heating results to be not as good as for $Cs_2NaYCl_6:Er^{3+}$. Besides concentration differences, our arguments are based on lack of overlap in absorption and emission and larger red shift in emission.

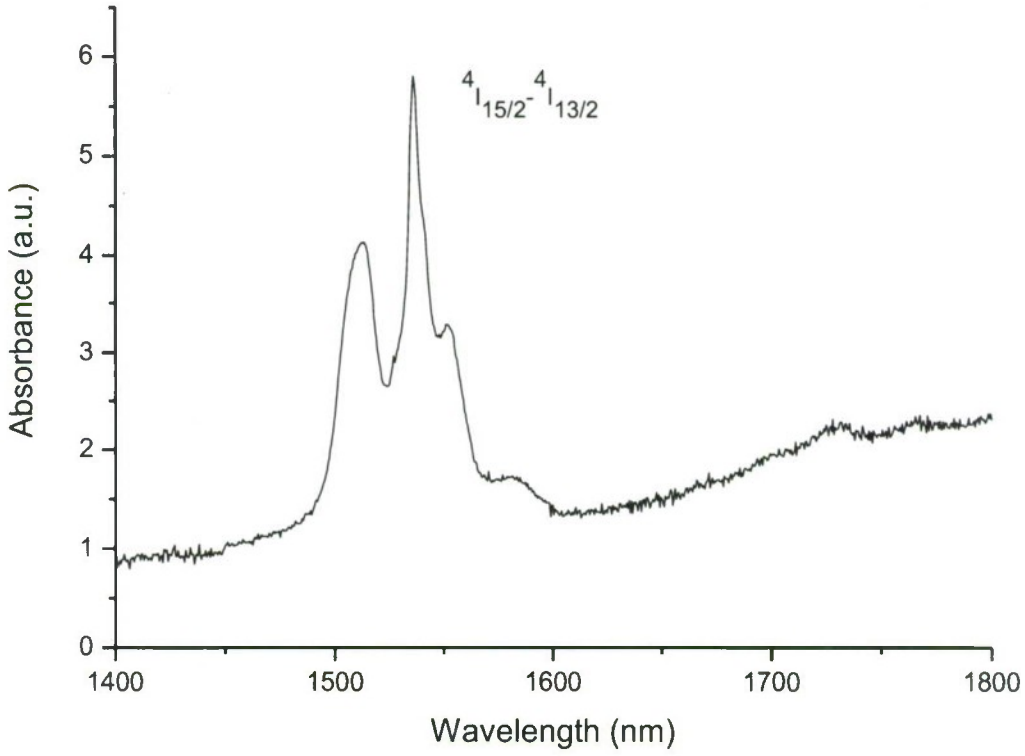

Figure 31. Room temperature absorption of $^4I_{15/2}$-$^4I_{13/2}$ in $KPb_2Cl_5:Er^{3+}$

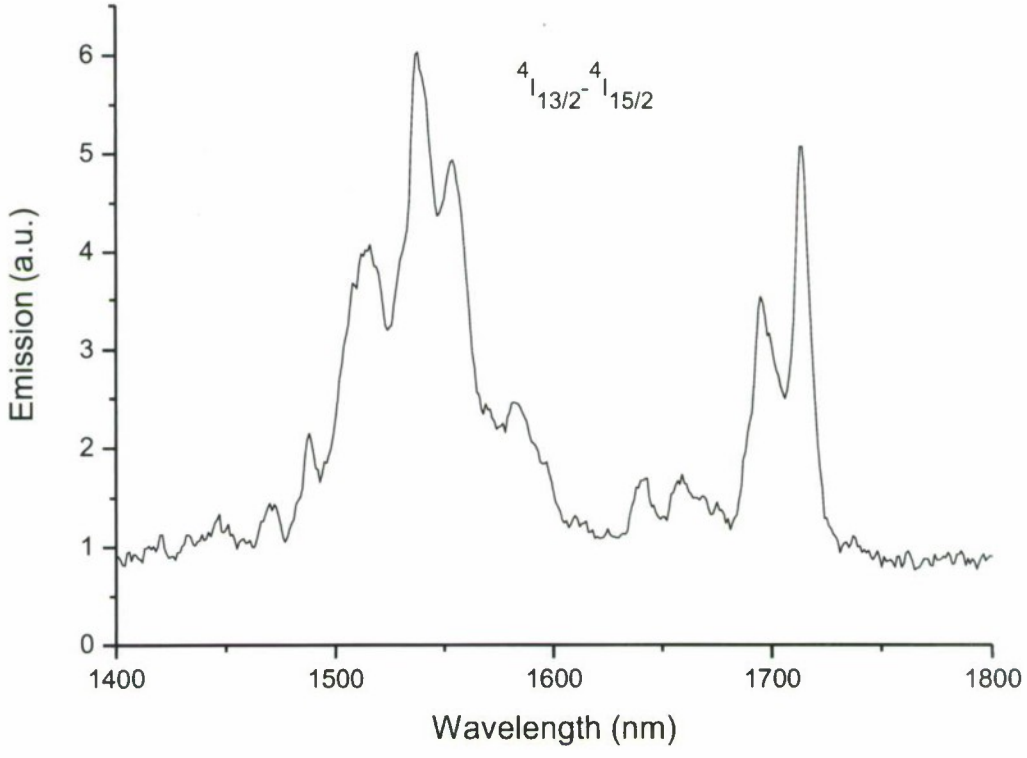

Figure 32. Room temperature emission of $^4I_{15/2}$-$^4I_{13/2}$ in $KPb_2Cl_5:Er^{3+}$

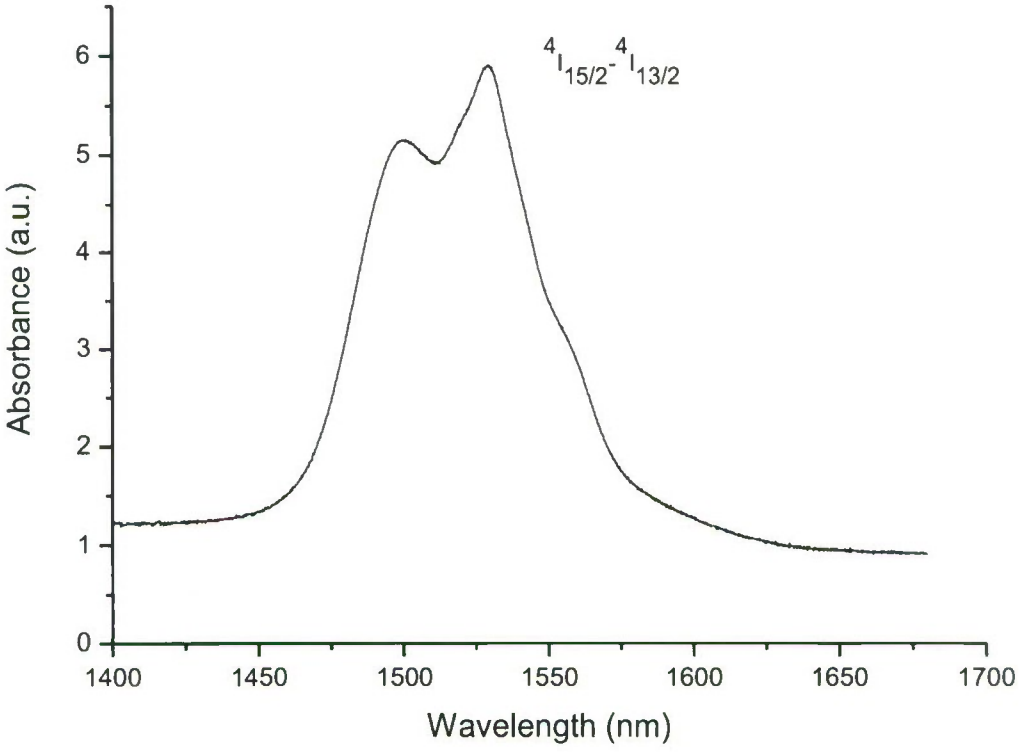

Figure 33. Room temperature absorption of $^4I_{15/2}$-$^4I_{13/2}$ in ZBLAN:Er^{3+}

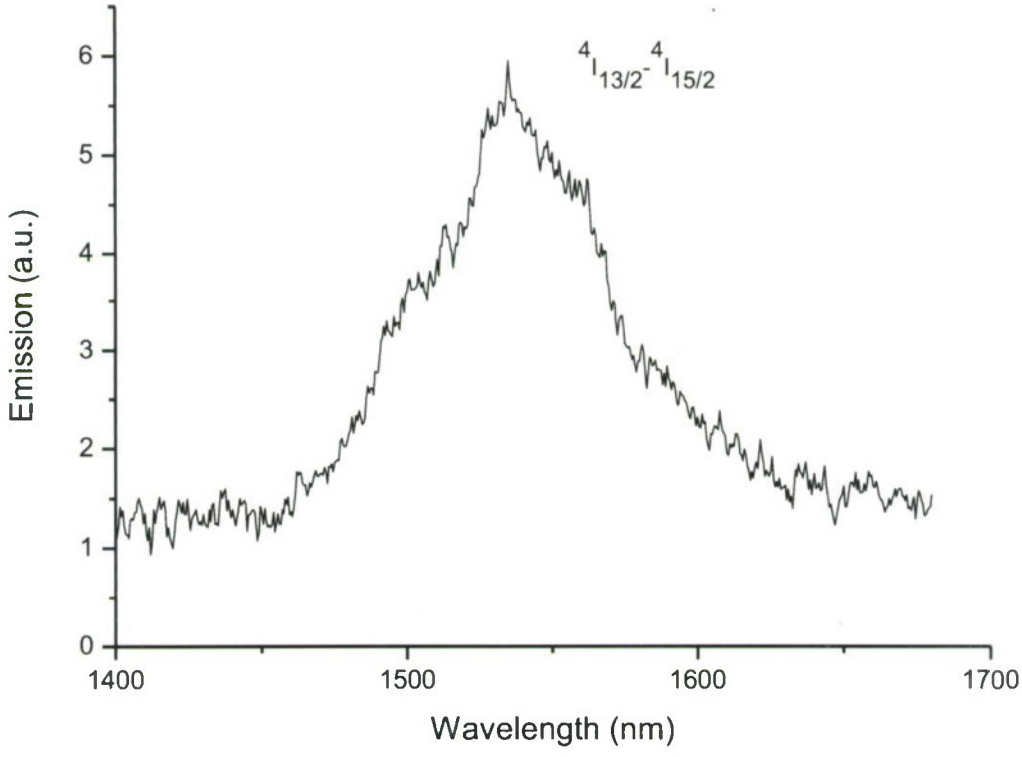

Figure 34. Room temperature emission of $^4I_{15/2}$-$^4I_{13/2}$ in ZBLAN:Er^{3+}

8.2.3 $^4I_{15/2}$ - $^4I_{13/2}$ 1.5 micron Cooling

So far in one system, $KPb_2Cl_5:Er^{3+}$ laser cooling at 1.5 micron has been reported. The cooling achieved was by a 0.03 K. We will compare the prospects of ZBLAN and $KPb_2Cl_5:Er^{3+}$ in this section and try to explain the low efficiencies and attainable temperature differences in cooling on the basis of spectroscopic data.

A comparison of emission spectra in the three hosts used here, Figures 19, 32 and 34 respectively, clearly shows striking differences. For $Cs_2NaYCl_6:Er^{3+}$ and ZBLAN, most of the intensity in absorption and emission is centered around 1.5 μm, whereas for $KPb_2Cl_5:Er^{3+}$ crystal, there is clearly another emission band centered around 1.7 μm. Therefore, pumping at λ=1567 nm would result in emission in the band lying at much lower energy, 1.7 μm. This will contribute to very significant non-radiative losses and will generate phonons and therefore heat the crystal.

The origin of the band centered at 1.7 microns that contributes to crystal heating is in the splittings of the ground $^4I_{15/2}$ and the excited $^4I_{13/2}$ states of Er. Even in cubic field, as seen in Figure 3, these states split by ~290 cm^{-1} and ~200 cm^{-1}, respectively. By the low symmetry crystal field of $KPb_2Cl_5:Er^{3+}$, the four fold degenerate Γ_8 states will further split into two Kramers doublets, Γ_6 and Γ_7, enhancing the span of $^4I_{15/2}$ – $^4I_{13/2}$ manifolds even more. Phonon energies at room temperature, added to these splittings, can result in the observed emission spectrum, Figure 32. The two main emission bands, centered at 1.73 μm and 1.6 μm, therefore, we assign as originating from two separated sets of crystal field states in $^4I_{13/2}$. These emissions also terminate to the well-separated crystal field states in the $^4I_{15/2}$ ground manifold. As the emission spectra of Cs_2NaYCl_6:Er and ZBLAN are very different from $KPb_2Cl_5:Er^{3+}$ and this

Stokes emission is not seen in there or in the cubic systems, we believe in case of KPb_2Cl_5, which has biaxial crystal symmetry, it is a consequence of entirely different transition selection rules.

The cooling efficiency using the 1.5 micron transition in the KPb_2Cl_5 host of Er is even lower than for 0.8 micron transition. This is a surprising result as the transition strength for $^4I_{15/2} - {}^4I_{13/2}$ is more than five orders of magnitude larger than for the $^4I_{15/2} - {}^4I_{9/2}$ transition. We attribute this to the excited state Stokes emission that will dominate after pumping in the 1570 nm range. Er^{3+}, due to its very complex and rich energy level structure extending from IR to UV, exhibits a variety of non-linear processes under intense excitation. The other reasons for the low efficiency of cooling like efficient non-radiative losses, upconversions, excited state absorptions and cross-relaxations should all be considered in detail to determine the efficiency of cooling. Such studies are currently in progress. In the presence of the energy level structure and radiative emission pathways that we have theoretically calculated and experimentally verified, the cooling efficiency should be extremely low if one pumps in the 1567 nm range. This is the only way one can explain the low efficiency and cooling, by only ~0.03 K, reported by Condon et al.

Our studies show that low efficiencies could only be true for the KPb_2Cl_5 host, and higher efficiencies of cooling can be seen in those systems where Stokes emissions are minimized. Our data shows that cubic Elpasolite hosts, $Cs_2NaYCl_6:Er^{3+}$, and ZBLAN are better suited for such studies. More so is the case of $Cs_2NaYCl_6:Er^{3+}$ that can accommodate up to 100% Er allowed by its formula and for that reason has shown far better cooling at 0.8 micron. Cooling experiments on these systems using 1.5 micron transition, i.e., $^4I_{15/2} - {}^4I_{13/2}$, are the next natural steps of our investigation.

9. Conclusions

The conclusion of this study is that erbium is a serious contender for an activator for laser refrigeration of solids.

Prior to this proposal it was believed that erbium would not exhibit optical cooling. With this grant a comprehensive research program was executed for atomically tailoring rare earth, especially erbium doped materials for laser refrigerators. It included fully quantum mechanical calculations for the energies and laser absorption strengths, fabricating the material and performing all characterization and laser cooling experiments in one laboratory. This multi-dimensional effort provided latitude in defining and refining the properties of the materials to be studied. The other conclusions of these studies are:

- As of the date of this report we have achieved temperature lowering more than 6 K from room temperature in bulk material using the 0.8 micron transition of erbium. This is an order of magnitude or two better than the cooling temperatures achieved previously in erbium based solids. However, it is not low enough for applications in optical cooling. Research on lowering this temperature limit is therefore very promising; especially due to the fact that the transition reported here is the weakest optical transition of erbium.
- The 1.5 micron transition of erbium shows almost a million times stronger absorption strength experimentally as was predicted by our calculations. This transition with proper tailoring in stoichiometric material has the greatest potential for cooling. Investigations on this transition are currently underway.
- Elpasolites with high concentration of erbium provided the best cooling results reported so far for erbium based materials, more than 6 K bulk temperature reduction. These

studies showed the importance of stoichiometric materials that can incorporate up to 100% rare earth concentration possible by chemical formula.

- Using stoichiometric materials, the thickness of the laser cooling medium can be reduced by two orders of magnitude or more. This implies that thinfilm laser cooling devices could become viable in the future.
- The quantum mechanical calculations for optical properties of rare earth materials provide a definitive parameter extraction into the working of a material as a suitable medium for laser refrigeration. Calculations on cubic systems studied here proved to be very accurate in predicting the experimental results.
- Erbium chloro-elpasolites, the crystals used in these investigations were highly reactive with water traces in the environment. To improve upon this material we recommend substituting it with a non-reactive but stoichiometric material.

This report makes a case for erbium based solid state materials to be atomically tailored for better and compact laser refrigerators. This could bring cooling down to 15 K or even lower temperatures especially using the 1.5 micron transition.

10. Recommendations

We recommend that erbium based stoichiometric materials in the form of single crystals, thinfilms and nano-compacted materials be investigated for efficient laser cooling down to liquid helium temperature. This, we recommend, can be achieved by using the 1.5 micron transition of erbium and atomically tailoring it to yield efficient low temperature cooling.

The cryogenic temperature of operation is the biggest obstacle to the successful implementation of many developing technologies. In the past decade one successful example where antistokes fluorescence cooling was readily employed was in the realization of radiation balanced lasers that require no external cooling in spite of their high power. The cooling of the lasing medium is achieved by the antistokes process inherent in laser action [50-55]. The need for cryogenic temperatures is even stronger for futuristic technologies such as spectral memories and quantum computing that offer even more compact devices [56-60]. Currently, the operational temperature of optical coolers has reached 150 K. Therefore, another order of magnitude lower temperature is necessary to reveal the full potential of laser cooling. The dividends of this technology include compact optical refrigerators which will not only set a new paradigm of miniaturization for technologies in the decades to come, but will also set new standards for making cryogenic science energy efficient and affordable globally.

Research performed under this program has opened a new avenue in laser cooling studies. It has shown that erbium based solids can be laser cooled using antistokes florescence. Erbium is a well tested and established rare earth ion that has provided lasers and amplifiers for communication and other technologies. Laser cooling has been reported using two transitions of

erbium, one in the near infrared, 0.8 micron, and the other in the eye safe region at 1.5 microns. To fully exploit the potential of erbium based solid state systems we recommend the following:

- We recommend using stoichiometric systems where erbium can be incorporated with high concentrations to increase cooling efficiency. This study has included systems up to eighty percent of erbium allowed by chemical formula.
- We recommend using the $^4I_{15/2}$ - $^4I_{13/2}$ transition of erbium that is in the eye safe region in stoichiometric solids for laser cooling. Very low efficiencies of cooling have been already reported for this transition in crystals containing low concentrations of erbium, i.e., a fraction of a percent or less. It is expected that in properly tailored stoichiometric systems the efficiency of cooling can be enhanced by several orders of magnitude.
- We recommend atomic tailoring of the erbium wavefunctions and hence, transition strengths in different crystals. This will lead to enhanced cooling efficiency and lower attainable temperatures.
- We recommend that erbium ground state energies be tailored to achieve lower temperatures of cooling. Erbium allows for multiple low energy crystal field states in the ground manifold that can be tailored by changing the crystal field. Such low lying states are necessary for low temperature cooling in rare earth based systems. It is estimated that in comparison to other rare earths, erbium can provide cooling down to a few degrees Kelvin.
- We recommend nano-compacted materials be investigated. These materials facilitate low energy phonons and will increase efficiency and provide lower temperatures of laser cooling.

- We recommend thinfilm structures be investigated in stoichiometric systems. The cooling power of thinfilm structures can be very high, several orders of magnitude higher than non-stoichiometric system. Therefore, thinfilms of such materials can provide sufficient cooling power in particular for applications where the materials to be cooled are in the form of thinfilm arrays of sensors, diodes or other electronic or photonic devices. Laser cooling in thinfilm has the attractive feature of minimizing radiation re-trapping. Specifically, as the antistokes shifted photon is emitted it can be re-trapped by another rare earth ion that can subsequently result in creating more phonons and heating the solid. Thinfilm laser refrigerators would greatly reduce the re-trapping cross-section.

11. References

[1] P. Pringsheim, *Z. Phys.* **57**, 739 (1929)

[2] S. Vavilov, *J. Phys.* (Moscow) **9,** 68 (1945)

[3] S. Vavilov, *J. Phys.* (Moscow) **10,** 499 (1946)

[4] L. Landau, *J. Phys.* (Moscow) **10,** 503 (1946)

[5] T. Kushida, and J.E. Geusie, *Phys. Rev. Lett.* **21**, 1172 (1968)

[6] I. Tsujikawa and T. Murao, *J. Phys. Soc. Jpn.* **18**, 206 (1963)

[7] D. F. Nelson and M.D. Sturge, *Phys. Rev. A.*, 137, 1117 (1965)

[8] R. I. Epstein, M. I. Buchwald, B. C. Edwards, T. R. Gosnell, and C. E. Mungan, *Nature* **377** (1995)

[9] J. Thiede, J. Distel, S. R. Greefield and R.I. Espstein, *Appl. Phys. Lett.* **86**,154107 (2005)

[10] C. E. Mungan, M. I. Buchwald, B. C. Edwards, R. I. Epstein, and T. R. Gosnell, *Appl. Phys. Lett.* **71**, 1458 (1997)

[11] G. Lamouche, P. Lavallard, R. Suris, R. Grousson, *J.Appl. Phys.*, **84** 509 (1998)

[12] B. C. Edwards, J. E. Anderson, R. I. Epstein, G. L. Mills, and A. J. Mord, *J. Appl. Phys.* **86**, 6489 (1999)

[13] C.E. Mungan, and T.R. Gosnell, *Adv. At. Mol. Opt. Phys.* **40**, 161 (1999)

[14] T. R. Gosnell, *App. Opt.* **24**, 1041 (1999)

[15] C. W. Hoyt, M. Sheik-Bahae, R. I. Epstein, B. C. Edwards, and J. E. Anderson, *Phys. Rev. Lett.* **85**, 3600 (2000)

[16] J. Fernandez, A. Mendioroz, A. J. Garcia, R. Balda, and J. L. Adam, *Phys. Rev. B* **62**, 3213 (2000)

[17] S. R. Bowman and C. E. Mungan, *Appl. Phys. B* **71**, 807 (2000)

[18] A. Rayner, M. Hirseh, N. R. Heckenberg, and H. Rubinsztein-Dunlop, *App. Opt.* **40**, 5423 (2001)

[19] R. I. Epstein, J. J. Brown, B. C. Edwards, and A. Gibbs, *J. Appl. Phys.* **90**, 4815 (2001)

[20] A. Mendioroz, J. Fernandaz, M. Voda, M. Al-Saleh, and R. Balda, *Opt. Lett.* **27**, 15 (2002)

[21] M. Sheik-Bahae and R. I. Epstein, *Nature Photonics,* **1**, 693 (2007)

[22] M. Sheik-Bahae (Private Communieations)

[23] J. Fernandez, A. J. Gareia-Adeva, and R. Balda, *PRL*, **97**, 033001 (2006)

[24] N.J. Condon, S.R. Bowman, S.P. O'Connor, R.S. Quimby and C.E. Mungan, *Optics Express*, **17**, 5466 (2009)

[25] R.I. Epstein (Private Communieations)

[26] Z.Hasan and F. S. Riehardson, *Mol. Phys.* **45**, 1299 (1982)

[27] A. De Piante, F. S. Riehardson and Z. Hasan, *J. Chem. Phys.* **82**, 1102 (1985).

[28] Karl A. Sehoene, Z. Hasan, John R. Quagliano and F. S.Riehardson, *Inorg. Chem.* **30**, 3813 (1991)

[29] Z. Hasan, L. Biyikli, M. J. Sellars, G. A. Khodaparast and F. S. Riehardson, *Physical Review B* **56**, 4518 (1997)

[30] S. Huffner, *Optical Spectra of Transparent rare earth Compounds* (Academie Press, Inc., New York, NY 1978)

[31] M.F. Aly, L. Biyikli, S. Dardona, J.L. Park and Z. Hasan, *SPIE Proceedings on Photonic Devices and Algorithms for Computing*, **4114**, 182 (2000)

[32] S. M. Syedahmedian, M.F. Aly, L Biyikli, J.L Park, M. Solonenko, and Z. Hasan, *J.Lumin.* **84**, 389 (1999)

[33] Z. Hasan and L. Biyikli, *Materials Science Forum* **315**, 51 (1999)

[34] Z. Hasan, S. Dardona and A. Konjhodzie, *J. Chem. Phys.* **123**, 224715 (2005)

[35] Z. Hasan, F. Bezares, J. Park, M. Campanell, M. Aly, *SPIE Proceedings on Photonic Devices and Algorithms for Computing*, **6482**-04-1, (2007)

[36] F. Bezares and Z. Hasan (to be published)

[37] A. S. Barker and A. J. Sievers, *Rev. Mod. Phys.* **47**, S1 (1975)

[38]S. A. FitzGerald, A. J. Sievers, and J. A. Campbell, *J. Phys.: Cond. Matt.***13**, 2095 (2001)

[39] N. J. Coekroft, G. D. Jones, and D. C. Nguyen, *Phys. Rev.* **B 45**, 5187 (1992)

[40] C. Campochiaro, C. D. Flint, Z. Hasan, G. Holingsworth, N.B. Manson, and D.S. McClure, *J. Lumin.*, **60**, 684-687 (1994)

[41] C. Campochiaro, C. D. Flint, Z. Hasan, G. Holingsworth, and D. S. McClure, *J. Lumin.*, **58**,1-4 (1994)

[42] A. De Piante, F. S. Richardson and Z. Hasan, *J. Chem. Phys.*, **82**, 1102-1111 (1985)

[43] Z. Hasan and N. B. Manson, *Mol. Phys.* **40,** 1227-1248 (1980)

[44] H. H. Patterson, Z. Hasan and N. B. Manson, *Chem. Phys. Lett.* **75**, 156-161 (1980)

[45] Z. Hasan and N. B. Manson, *J. Phys. C: (Sol. St. Phys.)* **12**, L269-272 (1979)

[46] J. B. Gruber, J. R. Quagliano, M. F. Reid, F. S. Richardson, M. E. Hills, M. D.Seltzer, S. B. Stevens, C. A. Morison, and T. H. Allik, *Phys.Rev.* B **48**, 15 561 (1993)

[47] W. T. Carnall, G.L. Goodman, K. Rajnak, and R.S. Rana, *J.Chem. Phys.* **90**, 3443 (1989)

[48] J. R. Quagliano, N. J. Cockroft, K. E. Gunde, and F. S. Richardson, *J.Chem. Phys.* **105**, 9812 (1996)

[49] E. G. Ettinger and T. M. Niemczyk, *J.Chem. Phys.* **68,** 872 (1978)

[50] L.R. Morss, M. Siegel, L. Stinger and N. Edelstein, *Inorg. Chem.* **9**, 1771 (1970)

[51] S. R. Bowman and Carl Mungan, in *Trends in Optics and Photonics*, edited by H. Injeyan, U. Keller, and C. Marshall (Opt. Soc. of Am., Washington DC 2000), Vol 34, p. 446-453

[52] N.W. Jenkins, S.R. Bowman, L.B. Shaw, and J.R. Lindel, *J. Lumin.*, **97**, 127 (2002)

[53] J. Ganem, J. Crawford, P. Schmidt, N. W. Jenkins, and S. R. Bowman, *Phys. Rev B* **66**, 1 (2002)

[54] S.R. Bowman, N.W. Jenkins, S. O'Connor and B.J. Feldman, *IEEE J. Quant. Elec.*, **38**, 1339 (2002)

[55] N.W. Jenkins, S.R. Bowman, S. O'Connor, S. K. Searles, and Joseph Ganem, *Opt. Mat.* **22**, 311 (2003)

[56] Z. Hasan, L. Biyikli, and P. I. Macfarlane, *App. Phys. Letters,* **72**, 3399 (1998)

[57] Z. Hasan, M. Solonenko, P. I. Macfarlane, L. Biyikli, V. K. Mathur and F.A. Karwacki, *App. Phys. Lett.* **72**, 2373 (1998)

[58] Z. Hasan and L Biyikli, *Journal of Optical Society of America* B, **18**, 232 (2001)

[59] Z. Hasan and V.K. Mathur, *U.S. Patent Numbers:* 6,528,234 (2003)

[60] V.K. Mathur and Z. Hasan, *U.S. Patent Numbers:* 6,514,435 (2003)

12. Symbols, Abbreviations, Acronyms

ZBLAN	A glass host consisting of ZrF_4-BaF_2-LaF_3-AlF_3-and NaF
ZBLANP	A glass host consisting of ZrF_4-BaF_2-LaF_3-AlF_3-NaF and PbF_2
CNBZn	A glass host consisting of CdF_2-$CdCl_2$-LaF_3-NaF-BaF_2-$BaCl_2$- and ZnF_2
Elpasolite	A crystal of the cubic structure named after the location where it mined for the first time.
RE	Rare earth atoms of the periodic table
Lanthanides	4f- rare earth elements of periodic table
Γ_6, Γ_7, and Γ_8	Electronic states in a cubic crystal
PMT	Photomultiplier tube
IR	Infrared
UV	Ultraviolet

13. Publications

13.1 Refereed Articles

1. Z. Hasan, S. Dardona and A. Konjhodzic, "Photolumiscence and Spectral Holeburning in Europium-Doped MgS Nanoparticles" *J. Chem. Phys.* **123**, 224715 (2005)
2. Z. Hasan, A. Konjhodzic, A. Adamczyk , F. Vagizov, E. E. Alp, W. Sturhahn, J. Zhao and J.J. Carroll, "Nuclear forward Scattering vs. Conventional Mossbauer Studies of Atomically Tailored Eu-Based Materials" *Hyperfine Interactions*, 170, 83 (2006)
3. Z. Hasan and A. Konjhodzic, "Microcharacterization of Spectral Memory Materials Using Nuclear Forward Scattering" *Proc. Of SPIE Vol. 6482*;08:1-8 (2007)
4. Z. Hasan,"Challenges for Ultra-Dense Spectral Memories" *Proc. Of SPIE Vol. 6903*;1-9 (2008)
5. F. Bezares and Z. Hasan, "Electron Microscopy and Spectroscopy of Thinfilms for Spectral Storage" *Proc. Of SPIE Vol. 6903*;1-9 (2008)
6. Z. Hasan, A. Konjhodzic, F. Bezares, A. Adamczyk and M. Aly, "Fabrication and Plasma Spectroscopy of Thinfilms for Power-Gated Holeburning" *Proc. Of SPIE Vol. 6482*;04:1-8 (2007)
7. Z. Hasan, J. Park, F. Bezares and Levent Biyikli, "Atomic Tailoring for Ultra-Dense Multi-layer Spectral Memories" *Proc. Of SPIE Vol. 6130*, 01:1-8 (2006)
8. Z. Hasan and Z. Qiu, "Atomic Tailoring of Rare Earth Based Materials for Laser Refrigeration" *Proc. Of SPIE Vol. 6130*, 0O:1-10 (2006)
9. Z. Hasan and Z. Qiu, J. Johnson, U. Homerick, "Optical characterization and crystal field calculations for some erbium based solid state materials for laser refrigeration" *Proc. Of SPIE Vol. 7228*, 72280H:1-12, (2009)

13.2 Edited Proceedings

1. Advanced Optical Concepts in Quantum Computing, Memory, and Communication II

   Editors: Zameer U. Hasan, Alan E. Craig, Philip R. Hemmer

   Published 4 February 2009

2. Advances in Photonics of Quantum Computing, Memory, and Communication III

   Editors: Zameer U. Hasan, Alan E. Craig, Philip R. Hemmer, et al.

   Published 8 February 2010

3. Advanced Optical and Quantum Memories and Computing III

   Editors: Hans J. Coufal, Zameer U. Hasan, Alan E. Craig

   Published 24 February 2006

4. Advanced Optical and Quantum Memories and Computing IV

   Editors: Zameer U. Hasan, Alan E. Craig, Selim M. Shahriar, et al.

   Published 7 February 2007

5. Advanced Optical Concepts in Quantum Computing, Memory, and Communication

   Editors: Zameer U. Hasan, Alan E. Craig, Philip R. Hemmer

   Published 29 January 2008

13.3 Publications in Progress

1. Bulk Laser Cooling in High Concentration Erbium Based Solids, Z. Hasan, Z. Qiu and J. Lynch
2. Stoichiometric Materials for Optical Refrigeration of Solids, Z. Hasan, Z. Qiu and J. Lynch

3. Crystal Field Analysis of Laser Cooling Transitions in the Near IR of Erbium in Different Hosts, Z. Hasan, Z. Qiu and J. Lynch
4. Atomic Tayloring of Multi-Layer Structures of Rare Earth Doped Solids for Speetral Storage, F. Bezares, J. Park, M. Aly and Z. Hasan
5. Seleetive Diffusion of Rare-Earth Impurities in PLD Thinfilms of CaS and MgS, F. Bezares, J. Park, S. Dardona, M. Syed and Z. Hasan
6. Nuelear Forward Scattering and Mossbauer Studies of Atomically Tailored Eu-Doped MgS Materials, Z. Hasan, A. Konjhodzie, A. Adamczyk , F. Vagizov, E. E. Alp, W. Sturhahn, J. Zhao
7. Nuclear Forward Scattering as a Tool for Nano-Charaeterization of Low Impurity Concentration Eu-Doped Materials, Z. Hasan, A. Konjhodzic, A. Adamczyk , F. Vagizov, E. E. Alp, W. Sturhahn, J. Zhao
8. Arrays of Optically Active Impurity-doped Nano-Particles on Silicon Matrix, Z.Hasan, A. Konjhodzic and R. Register

13.4 Invited Addresses and Lectures

Over 15 invited papers and presentations were made in the conferenees and academic institutions nationally and internationally.